



PAPER

OPEN ACCESS

RECEIVED

24 September 2020

REVISED

14 December 2020

ACCEPTED FOR PUBLICATION

5 January 2021

PUBLISHED

26 February 2021

Original content from this work may be used under the terms of the [Creative Commons Attribution 4.0 licence](#).

Any further distribution of this work must maintain attribution to the author(s) and the title of the work, journal citation and DOI.



From molecular quantum electrodynamics at finite temperatures to nuclear magnetic resonance

Kolja Them

Section Biomedical Imaging, Molecular Imaging North Competence Center (MOIN CC), Department of Radiology and Neuroradiology, University Medical Center Schleswig-Holstein and Kiel University, Am Botanischen Garten 14, 24118 Kiel, Germany

E-mail: kolja.them@rad.uni-kiel.de

Keywords: Molecular Quantum Electrodynamics at finite temperatures, Nuclear Magnetic Resonance, Numerical calculations, Return to equilibrium, Non-equilibrium real-time spin dynamics, Spin Boson System, Operator Algebras

Abstract

The algebraic reformulation of molecular Quantum Electrodynamics (mQED) at finite temperatures is applied to Nuclear Magnetic Resonance (NMR) in order to provide a foundation for the reconstruction of much more detailed molecular structures, than possible with current methods. Conventional NMR theories are directly related to the effective spin model, which idealizes nuclei as fixed points in a lattice \mathbb{Z}^3 . However, the delocalization of spins due to the thermal energy is more realistically described by the amplitude square of the nuclear wave function $|\Psi^\beta(X)|^2$ with $X \in \mathbb{R}^{3n}$, instead of fixed points in \mathbb{Z}^3 . In addition, the phenomenological integration of thermalization only allows an investigation of the molecular structure based on the position of the punctiform center of an NMR signal, but not based on the width and shape of NMR signals. Hence, a lot information on molecular structures remain hidden in experimental NMR data. In this document it is shown how $|\Psi^\beta(X)|^2$, $X \in \mathbb{R}^{3n}$ can be reconstructed from NMR data. To this end, it is shown how NMR spectra can be calculated directly from mQED at finite temperatures without involving the effective description. The new method connects all data points—the positions, widths, heights and shapes—of NMR signals directly with the molecular structure, which allows more detailed investigations of the underlying system. Furthermore, it is shown that the presented method corrects wrong predictions of the effective spin model. The fundamental problem of performing numerical calculations with the infinite-dimensional radiation field is solved by using a purified representation of a KMS state on a W^* -algebra. It is outlined that the presented method can be applied to any molecular system whose electronic ground state can be calculated using a common quantum chemical method. Therefore, the presented method can replace the effective description which forms the basis for NMR theory since 1950.

1. Introduction

Advances in chemistry, pharmacy, structure-based drug design and nanoscience often depend on the detailed knowledge of a molecular structure, which is determined by the spatial distribution of the nuclei [1]. In particular, the pharmacological properties of drugs depend heavily on small details of the charge distribution in the molecular structure [2]. In 1946, the experimental technique of Nuclear Magnetic Resonance (NMR) spectroscopy was developed, which is nowadays one of the most used and most advanced methods for molecular structure determination [3, 4]. NMR data contain highly detailed information on the spatial distribution of the nuclei including binding lengths, binding angles, bond rotations, molecular vibrations, proton exchange and the electronic influence of neighboring molecules [5]. From 1950 to 1953 Norman Ramsey calculated the chemical shift observed in NMR from the energy of the ground state, equation (2), and thus laid a foundation for today's NMR theory for structural analysis [6–9]. However, even 74 years after the invention of NMR, much information about molecular structures cannot be decoded and remains hidden in experimental NMR data.

This concerns especially molecular structures where the positions of the nuclei cannot adequately be described as fixed points in space. Due to the finite temperature the nuclei of a molecule are generally distributed in space to all positions which are accessible through thermal energy. Such delocalization is made possible in particular by bond rotations, molecular vibrations and proton exchange. Thus, a change of the temperature causes interconversions of superpositions of different conformations of a molecule. This has two effects on NMR signals, which typically have the shape of a Lorentz function: The position as well as the width (shape) of the NMR signal is influenced [10–12]. Delocalization of protons due to exchanging protons shows both effects on the signals as well. While the effects on the position of the signal can be investigated based on the electronic structure using modern methods of quantum chemistry [6, 13], modern NMR theory is so far unable to directly connect the shape of the NMR signals with the electronic structure [14–17]. Conventional NMR theory used for line shape analysis is highly phenomenological and mainly based on notions of Classical Physics. For example, bond rotations are described such that the nuclei rotate with a certain frequency and hence have time-dependent positions. Such concepts are integrated in conventional NMR theory in the form of rate constants. This is similar for proton exchange. However, in the more realistic theory of Quantum Statistical Mechanics bond rotations are included in wave functions Ψ^β whose amplitude square $|\Psi^\beta(X)|^2$ provides the *continuous probability distribution* to find the nuclei with conformation X . Thus, the description of delocalized nuclei using a spatial probability distribution $|\Psi^\beta(X)|^2$ is obviously more realistic and more detailed compared to an idealization as fixed point particles in combination with phenomenological rate constants.

However, conventional NMR theories are based on or are directly related to the effective spin model, equation (1), which idealizes nuclei as point particles at fixed positions x_i and whose thermal states are almost independent from the temperature [6–9]. The effective spin model had certainly great success over the last decades [18], but it also suffers from the fact that delocalization of nuclei due to bond rotations, vibrations and proton exchange can only be included phenomenologically [19, 20]. The phenomenological description in the form of rate constants gives a rough insight into these effects [21], but it also prevents a desirable analysis of the more realistic, continuous probability density $|\Psi^\beta(X)|^2$ for the spatial distribution of the nuclei. The effective model [22, 23]

$$H_{\text{eff}} = -\sum_i \gamma_i \vec{I}_i (\hat{1} - \sigma_i) \vec{B}_{\text{ext}} + 2\pi \sum_{i < j} J_{ij} \vec{I}_i \cdot \vec{I}_j + \sum_{i < j} \vec{I}_i D_{ij} \vec{I}_j, \quad (1)$$

contains the magnetic shielding σ_i , which is caused by surrounding electrons. The magnetic moments of these electrons show into the opposite direction of the external magnetic field and hence weakens the external field at the position of a nucleus. The indirect spin-spin couplings J_{ij} are also caused by electrons and enable energy exchange between nuclei at i and j . The tensor D_{ij} describes the magnetic dipole-dipole interactions between the nuclear spins \vec{I}_i and \vec{I}_j , \vec{B}_{ext} is a classical, external magnetic field and γ is the gyromagnetic ratio [6, 24]. In the most widely used approach the effective parameters are calculated according to second order derivatives of the ground state energy (Taylor-expansion) [6–9, 25]:

$$\sigma_i^{\alpha\delta} = \frac{\partial^2 E_0}{\partial \mu_i^\alpha \partial B^\delta} \quad \text{and} \quad J_{ij}^{\alpha\delta} = h \gamma_i \gamma_j \frac{d^2 E_0}{d \mu_i^\alpha d \mu_j^\delta}, \quad \alpha, \delta = x, y, z. \quad (2)$$

During the last decades there were done many works on the optimization of equation (2) by including relativistic [26–28] and QED effects [29–32] to the effective NMR parameters. Also numerically more efficient alternatives were introduced [33, 34]. All these effects are integrated in the form of corrections to the effective parameters σ and J and are therefore still inside the effective description which possesses a *discrete energy spectrum*. This is the same for the integration of the temperature [13], where the corrections $\Delta^\beta \sigma$ and $\Delta^\beta J$ are calculated according to

$$\Delta^\beta \sigma = \int d^{3n} X |\Psi^\beta(X)|^2 \sigma(X) - \sigma_{\text{eq}} \quad \text{and} \quad \Delta^\beta J = \int d^{3n} X |\Psi^\beta(X)|^2 J(X) - J_{\text{eq}}. \quad (3)$$

Here Ψ^β is the nuclear wave function and σ_{eq} as well as J_{eq} are the values at the equilibrium geometry, which corresponds to the configuration of lowest energy of the potential energy surface (PSE) and can be calculated according to equation (2). The multiplication operators $\sigma(X)$ and $J(X)$ give just the values of the corresponding effective parameters for the positions (configuration) X of the nuclei. The values $\sigma(X)$ and $J(X)$ are calculated also according to equation (2) except that the configuration X is not the point of lowest energy in the PSE. Hence, this approach is able to analyze the impact of the temperature on the position of an NMR signal but not on the shape of an NMR signal. A detailed discussion on the similarity and differences of this approach to the presented approach is given in the [appendix](#). To this end, conventional NMR theory strongly requires phenomenology which does not connect the molecular geometry but phenomenological parameters with the line shape. We do not describe these methods here in detail but refer to the literature [15–17, 35]. In order to obtain any line shape of finite width from the Fourier transformation of the nuclear spin dynamics—as it is done in NMR experiments—thermalization of the nuclear spins must be contained in the calculated spin dynamics. However, the unitary dynamics generated by (1) has bad thermalization properties because the Hamiltonian has a discrete energy

spectrum. Small systems consisting of a few spins does not thermalize at all and larger systems thermalize only approximately in very specific cases [36]. In order to include return to equilibrium (thermalization) anyway [37] the von Neumann equation was modified phenomenologically by introducing relaxation superoperators Γ [38, 39]:

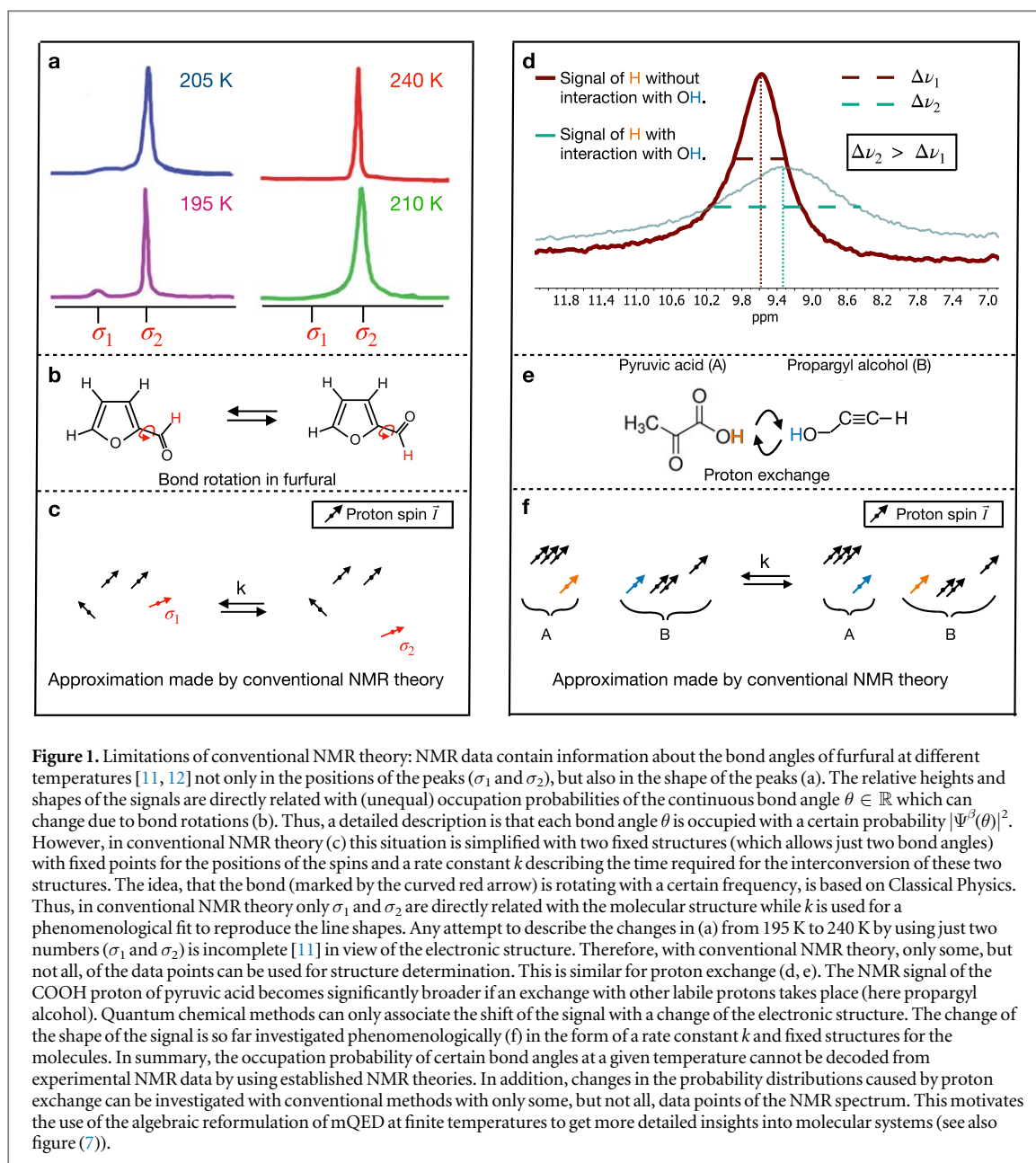
$$\frac{d\rho(t)}{dt} = -\frac{i}{\hbar}[H_{\text{eff}}, \rho(t)] - \Gamma(\rho(t) - \rho_0). \quad (4)$$

The final state ρ_0 to which the system shall evolve must be chosen "by hand". Certainly, it is preferable when the correct final state is an outcome and not an input of a theory. In all these methods, the microscopic origin of NMR line shapes is completely neglected and replaced by phenomenological parameters like rate constants k or relaxation parameters T_1 and T_2 . To conclude, in conventional NMR theory only some data points of the NMR spectrum—the positions of the NMR signals given by σ and J —are directly connected to the molecular geometry while the line shapes have so far no direct connection to the underlying molecular geometry. Line shapes are described phenomenologically. This is basically due to the fact that thermalization is included phenomenologically by equation (4) instead of coupling the spins to the quantized electromagnetic field at finite temperatures.

Illustrative examples where all data points—which means also the width of the NMR signals—contain important information on the underlying structure and were a description just in form of σ and J is incomplete are shown in figure 1 (a). In the real molecule (which is furfural in this example) all bond angles can be occupied via bond rotations (b). We know from quantum mechanics that every bond angle has a specific energy and the laws of thermodynamics provide the information about which of these bond angles are preferably occupied. Conventional NMR theory like the Bloch-McConnell equations, however, simplifies the molecule usually by using two different structures with fixed point positions for the nuclei and a rate constant k (left side (c) in figure 1). This rate constant describes the time required for the mutual conversion of these structures. Hence, the important information which bond angles are more and which are less preferred at a given temperature (compare also figure 7) cannot be decoded from experimental NMR data by using conventional NMR theory. This is because a description of the changes in the NMR spectrum just in terms of the positions of the NMR signals is incomplete. In the case of furfural, also the line shapes must be connected to the molecular structure in order to obtain a complete structure investigation. Otherwise not all details of the molecular structure can be decoded using conventional NMR theory such that they remain hidden in the experimental data. This is similar in the case of proton exchange (right side of figure 1, (d), (e) and (f)).

In this document it is shown how the probability distribution $|\Psi^\beta(X)|^2$ for the positions X of the nuclei can be analyzed and reconstructed from NMR spectra. To this end, it is shown how the NMR signal can be calculated *directly* from molecular Quantum Electrodynamics (mQED) at finite temperatures without using the effective spin model or effective NMR parameters. Hence, the presented method can be used to obtain a more detailed molecular structure from NMR data than currently possible with conventional NMR theory. Mathematically, this means that the lattice L , which serves for the restricted positions of the nuclei in the effective description, is replaced by the continuous space \mathbb{R}^3 in which the nuclei can be distributed continuously. A reconstruction of $|\Psi^\beta(X)|^2$ from NMR data is of special interest, because in most cases it is not possible to solve the nuclear Schrödinger equation. An outlook how a more detailed structure determination may look like is presented in section 8.

However, up to now it was not known how the spin dynamics can be calculated numerically when the spins interact with the infinitely dimensional, quantized electromagnetic field (EMF) with a *continuous* spectrum at finite temperatures. Two basic reasons for that are the occurrence of divergences in perturbation series and the infinite number of field quanta involved in finite temperature QED processes. In certain cases one may avoid the numerical and mathematical problems related to quantized fields at finite temperatures by using the ground state instead [40, 41]. However, in NMR at room temperature the nuclear spins are far away from their ground state and the temperature of the quantized electromagnetic field determines the temperature of the final state of the nuclear spins after equilibration [42]. Hence, the approach of using a ground state for the quantized EMF is obviously unsuitable for NMR at room temperature. There are several works on a method called Thermo Field Dynamics (TFD) [43–45] which is about quantized fields at finite temperatures. While this approach is widely used it also involves a large number of field quanta in the construction of the thermal vector state Ω^β . Furthermore, in TFD the state Ω^β is constructed using a *discrete* set of energy values E_n . An extension of the TFD methods to the continuous case is not possible. The use of a discrete energy spectrum for the quantized EMF and the limitation to a few (usually 1–100) frequencies is the common approximation made in current numerical methods. The discrete spectrum drastically simplifies the mathematical structure. No numerical method was found in the literature that uses a continuous energy spectrum for the quantized EMF to calculate the spin dynamics. However, as it turns out later in this document a discrete spectrum does not lead to satisfying results in the calculation of NMR spectra. Indeed, the incorporation of a continuous spectrum for the quantized EMF is



of paramount importance for the NMR line width which is directly related with return to equilibrium properties and determines the life time of excited spins. Hence, TFD is unsuitable for the calculation of NMR spectra.

In the present document the following problems for numerical methods are solved by using the mathematical structure from algebraic Quantum Field Theory [42, 46–51]:

- (I) Numerical calculations with the infinite-dimensional, quantized EMF at finite temperatures.
- (II) Numerical calculations with a continuous energy spectrum for the quantized EMF.
- (III) Convergence of the QED perturbation series.

Recent works investigated and avoided the occurrence of divergences by using appropriate smearing functions [42, 52, 53]. It remained to show which effect these restrictions have on expectation values, which will be done in this work. Recently, a perturbation series for interacting, massive quantum fields was constructed by Fredenhagen and Lindner [49]. This approach solved a long-standing problem and its extension to the Dirac field is of interest for relativistic effects from heavy nuclei in NMR. Further important structural developments were achieved in [54]. In this document it is shown that a purified form of the Araki-Woods representation [55], denoted by $(\mathfrak{H}_{AW}, \pi_{AW}^\beta)$, enables the numerical calculations involving bosonic fields at finite temperatures with striking advantages: In each order of the perturbation series at most one "Araki-Woods boson" is produced

while small coupling constants, connecting spins and the quantized electromagnetic field, reduce higher order contributions. The representation $(\mathfrak{H}_{\text{AW}}, \pi_{\text{AW}}^\beta)$ rigorously respects the continuous energy spectrum of the quantized electromagnetic field at finite temperatures and reduces the required computational resources for numerical calculations strongly. To summarize, this document shows that the application of the algebraic reformulation of mQED to NMR offers the following advantages over conventional NMR theory:

- (I) The drawback of a nearly temperature-independent initial state from which conventional NMR theory suffers (effective spin model) is repealed. Instead, the temperature-dependent probability density for the spatial distribution of the nuclei (the amplitude square of the nuclear wave function) can be used directly for the calculation of the spin dynamics.
- (II) In contrast to conventional NMR theory, the presented method directly connects all data points of the NMR spectrum with the molecular structure. This means that there is a direct and causal connection between NMR line shapes and the investigated molecular structure. Hence, no phenomenological parameters prevent the reconstruction of the spatial distribution of delocalized nuclei. This is due to the natural (not phenomenological) thermalization [42, 56] of the spin dynamics in mQED.
- (III) The above points (I) and (II) basically enable a much more detailed reconstruction of the molecular structure contained in NMR data than possible with established methods.
- (IV) Molecular rotations, vibrations and proton exchange are included in the probability density for the spatial distribution of the nuclei. Hence, the simplification that the positions of nuclei are restricted to fixed points is repealed in the calculation of the spin dynamics.

2. Molecular quantum electrodynamics

In order to use the perturbation theory developed by Araki, Bratelli, Robinson and Kishimoto the Hamiltonian will be separated into $H = H_0 + H_{\text{Int}}$. The physical system will be described by a combination of a Pauli-Fierz and a generalized Spin-Bose model in Coulomb gauge [52, 56]. The resulting molecular QED Hamiltonian is given by

$$H_0 = -\left(\sum_{j=1}^K \gamma_j \vec{I}_j + \sum_{i=1}^E \vec{\mu}_{ij}\right) \cdot \vec{B}_{\text{ext}} + \hbar \sum_{\lambda=1,2} \int_{\mathbb{R}^3} d^3k \omega(\vec{k}) a_\lambda^*(\vec{k}) a_\lambda(\vec{k}) + \sum_{i=1}^E \frac{\vec{p}_i^2}{2m_e} + \sum_{j=1}^K \frac{\vec{P}_j^2}{2M_j} + V(X^e, X) \quad (5)$$

and

$$H_{\text{Int}} = -\sum_{j=1}^K \gamma_j \vec{I}_j \cdot \vec{B}_\varphi(\vec{x}_j) + \sum_{i=1}^E \left(i \frac{e\hbar}{m_e} \vec{A}_\varphi(\vec{x}_i^e) \cdot \vec{\nabla}_i^e + \frac{e^2}{2m_e} (\vec{A}_\varphi(\vec{x}_i^e))^2 - \vec{\mu}_{ij} \cdot \vec{B}_\varphi(\vec{x}_i^e) \right). \quad (6)$$

The first term in H_0 couples the K nuclear spins \vec{I}_j and the E total magnetic moments $\vec{\mu}_{ij} = -\mu_B/\hbar (g_e \vec{s}_i + \vec{I}_i)$ of the electrons to the classical, external magnetic field \vec{B}_{ext} . For high field strengths of the external magnetic field, i.e., $B_{\text{ext}}^z > 3\text{T}$, spin-orbit couplings can be neglected due to the Paschen-Back effect. The second term describes the energy of the quantized, electromagnetic field. $a_\lambda^*(\vec{k})$ and $a_\lambda(\vec{k})$ are the common creation and annihilation operators with commutation relations

$$[a_\lambda(\vec{k}), a_{\lambda'}^*(\vec{k}')] = \delta(\vec{k} - \vec{k}') \delta_{\lambda, \lambda'}, \quad [a_\lambda(\vec{k}), a_{\lambda'}(\vec{k}')] = 0, \quad \text{and} \quad [a_\lambda^*(\vec{k}), a_{\lambda'}^*(\vec{k}')] = 0 \quad (7)$$

and with momentum $\vec{k} \in \mathbb{R}^3$ and polarization $\lambda = 1, 2$. The last three terms provide the non-relativistic Schrödinger-Operator. Thus, \vec{p}_i is the momentum operator of electron i , \vec{P}_j is the momentum operator of nucleus j and the potential $V(X^e, X)$ depending on coordinates X^e of E electrons and X of K nuclei is given by

$$V(X^e, X) = \sum_{i < j}^E \frac{e^2}{4\pi\epsilon_0 x_{ij}^e} - \sum_{i=1}^E \sum_{j=1}^K \frac{Z_j e^2}{4\pi\epsilon_0 \|\vec{x}_i^e - \vec{x}_j\|} + \sum_{i < j}^K \frac{Z_i Z_j e^2}{4\pi\epsilon_0 x_{ij}}. \quad (8)$$

Z_j is the number of protons in nucleus j , \vec{x}_i^e is the coordinate of electron i and \vec{x}_j of nucleus j . x_{ij}^e and x_{ij} are the distances between electrons or nuclei and the other constants can be found in the literature [57]. H_{Int} couples the independent terms and enables energy exchange between the nuclear spins and the rest of the system. We use the definition $\vec{A}_\varphi(\vec{x}_j) \doteq \vec{A}_{0,\varphi}(\vec{x}_j, 0)$ and for the quantized vector potential the free time evolution provides

$$\vec{A}_{0\varphi}(\vec{x}, t) = \sqrt{\frac{\hbar}{2\epsilon_0(2\pi)^3}} \sum_{\lambda=1,2} \int_{\mathbb{R}^3} d^3k \vec{\epsilon}_\lambda(\vec{k}) \frac{\varphi(\vec{k})}{\sqrt{\omega(\vec{k})}} (e^{-i(\vec{k}\vec{x}-\omega(\vec{k})t)} a_\lambda^*(\vec{k}) + e^{i(\vec{k}\vec{x}-\omega(\vec{k})t)} a_\lambda(\vec{k})). \tag{9}$$

The quantized magnetic field is given by $\vec{B}_\varphi = \vec{\nabla} \times \vec{A}_\varphi$ and we have

$$\vec{B}_{0\varphi}(\vec{x}, t) = i \sqrt{\frac{\hbar}{2\epsilon_0(2\pi)^3}} \sum_{\lambda=1,2} \int_{\mathbb{R}^3} d^3k (\vec{k} \times \vec{\epsilon}_\lambda(\vec{k})) \frac{\varphi(\vec{k})}{\sqrt{\omega(\vec{k})}} (e^{-i(\vec{k}\vec{x}-\omega(\vec{k})t)} a_\lambda^*(\vec{k}) - e^{i(\vec{k}\vec{x}-\omega(\vec{k})t)} a_\lambda(\vec{k})), \tag{10}$$

where $\varphi \in L^2(\mathbb{R}^3)$ is the coupling function with suitable IR and UV behavior [56–58] to prevent divergences in the individual terms of the perturbation series. The presented model is independent of a specific choice of the polarization vectors. Using the notation $x = (\vec{x}, t)$, $k = (\vec{k}, \omega(\vec{k}))$ and Einstein’s sum convention $k^\mu x_\mu = \vec{k} \cdot \vec{x} - \omega(\vec{k})t$ we have

$$[B_{0\varphi}^\alpha(x), B_{0\varphi}^\gamma(y)] = - \sum_{\lambda=1,2} \int d^3k \varphi_\lambda^\alpha(\vec{k}) \varphi_\lambda^\gamma(\vec{k}) i\Delta_{\vec{k}}(x - y) \tag{11}$$

with $\varphi_\lambda^\alpha(\vec{k}) \doteq (\sqrt{\hbar/\epsilon_0}) \varphi(\vec{k}) (\vec{k} \times \vec{\epsilon}_\lambda(\vec{k}))^\alpha$, $\alpha, \gamma = x, y, z$ and

$$i\Delta_{\vec{k}}(x - y) = \frac{e^{-ik^\mu(x-y_\mu)} - e^{ik^\mu(x-y_\mu)}}{(2\pi)^3 2\omega(\vec{k})}. \tag{12}$$

Since the commutator function is linked to the Feynman propagator we will have the interpretation for the probability for the propagation of field quanta between the nuclear spins located at x and y .

3. Algebraic quantum field theory

Operator algebras are central objects in the algebraic reformulation of Quantum Statistical Mechanics and Quantum Field Theory. Several structural elements of operator algebras are required for the numerical calculations in the application of mQED at finite temperatures to NMR. The most central objects of operator algebras are briefly reviewed from [46] and [47] before the Field Theory is described. Further mathematical structures that are required for the numerical calculations can be found in the [appendix](#).

Basics of Operator Algebras. The commutant of an algebra \mathfrak{A} is denoted by \mathfrak{A}' and we have $(\mathfrak{A}')' = \mathfrak{A}''$. The set of bounded operators on a Hilbert space \mathfrak{H} is denoted by $\mathfrak{B}(\mathfrak{H})$.

Definition 1. A von Neumann algebra on a Hilbert space \mathfrak{H} is a $*$ -subalgebra \mathfrak{M} of $\mathfrak{B}(\mathfrak{H})$ such that

$$\mathfrak{M} = \mathfrak{M}'' \tag{13}$$

The terminology W^* -algebra is often used for the abstractly defined algebra and then the name von Neumann algebra is reserved for the operator algebras. Note that a C^* -algebra is a closed set in the norm topology and a W^* -algebra is weakly closed. A bounded observable A is a selfadjoint element of a C^* - or a W^* -algebra \mathfrak{A} . A state ω is a positive, normalized, and linear functional on \mathfrak{A} , i.e., $\omega \in \mathfrak{A}^*$, where \mathfrak{A}^* is the dual of \mathfrak{A} . An expectation value is given by

$$\omega(A) = (\psi_\omega, \pi_\omega(A)\psi_\omega), \tag{14}$$

where $\pi_\omega: \mathfrak{A} \rightarrow \mathfrak{B}(\mathfrak{H})$ and $\psi_\omega \in \mathfrak{H}_\omega$. The index ω on ψ_ω , \mathcal{H}_ω and π_ω denotes the association of the representation $(\mathcal{H}_\omega, \pi_\omega)$ and the vector ψ_ω with the state ω . However, we will neglect this index for simplicity because no confusion can appear. The space \mathfrak{H}_ω is called the representation space and the operator examples $\pi(A)$ are called the representatives of \mathfrak{A} . A $*$ -isomorphism of an algebra \mathfrak{A} into itself is called a $*$ -automorphism τ . The time evolution of a physical system is given by a one-parametric group of $*$ -automorphisms τ_t , which is generated by a derivation δ . Thus, the derivation δ contains the information of the Hamiltonian H and one formally has $A \mapsto \tau_t(A) = e^{\frac{t}{\hbar}\delta}(A)$.

Definition 2. A W^* -dynamical system is a pair (\mathfrak{M}, τ) , where \mathfrak{M} is a W^* -algebra and $\tau: G \rightarrow \text{Aut}(\mathfrak{M})$, $G \ni g \mapsto \tau_g$ is a weakly continuous representation of a locally compact group G as $*$ -automorphisms acting on \mathfrak{M} .

Note that a C^* -dynamical system (\mathfrak{A}, τ) is defined in a similar fashion. In this case \mathfrak{A} is a C^* -algebra and τ is a strongly continuous representation of a locally compact group as $*$ -automorphisms acting on \mathfrak{A} . In order to proceed with equilibrium states we define the strip $S_\beta \doteq \{z \in \mathbb{C} | 0 < \Im(z) < \beta\}$.

Definition 3. Let (\mathfrak{A}, τ) be a C^* - or a W^* -dynamical system. A state ω^β on \mathfrak{A} , supposed to be normal in the W^* -case, is a (τ, β) -KMS state for some $\beta \in \mathbb{R}^+$ if the following holds. For any $A, B \in \mathfrak{A}$ there exist a function $F_\beta(A, B; z)$ which is analytic on the strip S_β , continuous on its closure and satisfies the Kubo–Martin–Schwinger

condition

$$F_\beta(A, B; t) = \omega^\beta(A\tau_t(B)) \quad \text{and} \quad F_\beta(A, B; t + i\beta) = \omega^\beta(\tau_t(B)A) \quad (15)$$

on the boundary of S_β .

Description of the field theory. A single photon is described as a square integrable function $f \in \mathfrak{H} = L^2(\mathbb{R}^3 \times \{1, 2\})$, $(\vec{k}, \lambda) \mapsto f_\lambda(\vec{k}) \in \mathbb{C}$ with momentum $\vec{k} \in \mathbb{R}^3$ and polarization $\lambda \in \{1, 2\}$. The Hilbert space \mathfrak{H} is called the 1-particle Hilbert space. The n-particle Hilbert space \mathfrak{H}^n is given by the n-fold tensor product of \mathfrak{H} with itself, i.e., $\mathfrak{H}^n = \mathfrak{H} \otimes \mathfrak{H} \cdots \otimes \mathfrak{H}$. The projection $P_+ \mathfrak{H}^n = \mathfrak{H}_+^n$ [47] onto totally symmetric n-particle wave functions reflects that the particles obey the Bose–Einstein statistics. The photon Fock-space is then defined by

$$\mathfrak{F}_+(\mathfrak{H}) = \bigoplus_{n=0}^{\infty} \mathfrak{H}_+^n. \quad (16)$$

with vacuum $\Omega_0 \in \mathfrak{F}_+(\mathfrak{H})$. The smeared creation and annihilation operators are defined by

$$a_\lambda^*(f_\lambda) = \int d^3k f_\lambda(\vec{k}) a_\lambda^*(\vec{k}) \quad \text{and} \quad a_\lambda(f_\lambda) = \int d^3k \overline{f_\lambda(\vec{k})} a_\lambda(\vec{k}) \quad (17)$$

for $f \in \mathfrak{H}$. $a_\lambda^*(\vec{k})$ and $a_\lambda(\vec{k})$ satisfy the commutation relations in equation (7), which translates to

$$[a_\lambda(f_\lambda), a_{\lambda'}(g_{\lambda'})] = \delta_{\lambda, \lambda'} \langle f_\lambda | g_{\lambda'} \rangle \quad \text{and} \quad [a_\lambda(f_\lambda), a_{\lambda'}(g_{\lambda'})] = [a_\lambda^*(f_\lambda), a_{\lambda'}^*(g_{\lambda'})] = 0 \quad (18)$$

with

$$\langle f_\lambda | g_\lambda \rangle = \int_{\mathbb{R}^3} d^3k \overline{f_\lambda(\vec{k})} g_\lambda(\vec{k}). \quad (19)$$

A field operator $\Phi(f)$ is given by

$$\Phi(f) \doteq \frac{1}{\sqrt{2}} \sum_{\lambda=1,2} (a_\lambda^*(f_\lambda) + a_\lambda(f_\lambda)) \quad (20)$$

and the notation for the quantized magnetic field in section II, equation (10), is recovered by $B_{0\varphi}^\alpha(\vec{x}, t) \equiv \Phi(b_{\varphi\lambda}^{\alpha(\vec{x}, t)})$ with $\alpha = x, y, z$. According to equation (10) the functions $b_{\varphi\lambda}^{\alpha(\vec{x}, t)}: \mathbb{R}^3 \rightarrow \mathbb{C}$ are given by

$$\vec{k} \mapsto b_{\varphi\lambda}^{\alpha(\vec{x}, t)}(\vec{k}) = i \sqrt{\frac{\hbar}{\epsilon_0(2\pi)^3}} (\vec{k} \times \vec{e}_\lambda(\vec{k}))^\alpha \frac{\varphi(\vec{k})}{\sqrt{\omega(\vec{k})}} e^{-ik^\mu x_\mu} \quad \text{and} \quad \alpha = x, y, z. \quad (21)$$

Since the field operators are unbounded one introduces the bounded Weyl operators

$$W(f) = \exp(i\Phi(f)), \quad \text{satisfying} \quad W(f)W(g) = e^{-i\mathcal{J}(\langle f | g \rangle)} W(f + g). \quad (22)$$

In order to rigorously define equilibrium states the one-particle Hilbert space has to be restricted by $\mathfrak{H}^r = \{f \in \mathfrak{H}; \omega^{-1/2}f \in \mathfrak{H}\}$, which ensures a suitable infrared behavior. This basically means to "reduce or neglect" extremely low energetic photons. However, in this document no infrared divergences were found in the numerical calculations and the restriction of $b_{\varphi\lambda}^{\alpha x}$ to \mathfrak{H}^r can be chosen such that the influence of the restriction on the expectation value is arbitrarily small. We define a C^* -algebra \mathfrak{A}_{EM} for the quantized electromagnetic field by

$$\mathfrak{A}_{EM} \doteq \mathcal{W}(\mathfrak{H}^r) = \overline{\text{span}\{W(f); f \in \mathfrak{H}^r\}}^{\|\cdot\|}, \quad (23)$$

where the closure is taken in the uniform norm $\|\cdot\|$ for bounded operators on the bosonic Fock space $\mathfrak{F}_+(\mathfrak{H}^r)$. The dispersion relation is given by $\omega(\vec{k}) = c|\vec{k}|$ where c is the speed of light and the free field Hamiltonian is given by

$$H_{EM} \doteq d\Gamma(\omega) \equiv \hbar \sum_{\lambda=1,2} \int_{\mathbb{R}^3} d^3k \omega(\vec{k}) a_\lambda^*(\vec{k}) a_\lambda(\vec{k}). \quad (24)$$

$d\Gamma(\omega)$ provides an infinitesimal generator δ_{EM} , formally given by $\delta_{EM} = [H_{EM}, \cdot]$, that generates the one-parameter group $\{\tau_t^{EM}\}_{t \in \mathbb{R}}$ for the quantized electromagnetic field.

The GNS-representation $(\mathfrak{H}_{AW}, \pi_{AW}^\beta)$ which is induced by the (τ^{EM}, β) -KMS state ω_{EM}^β on \mathfrak{A}_{EM} was found by Araki and Woods [55] and is therefore referred as Araki-Woods representation. The representation space is given by

$$\mathfrak{H}_{AW} = \mathfrak{F}_+(\mathfrak{H}^r) \otimes \mathfrak{F}_+(\mathfrak{H}^r), \quad (25)$$

the annihilation operators are given by

$$\pi_{AW}^\beta(a_\lambda(f_\lambda)) = a_\lambda(\sqrt{1 + \rho_\beta} f_\lambda) \otimes \hat{1} + \hat{1} \otimes a_\lambda^*(\sqrt{\rho_\beta} \vec{f}_\lambda) \quad (26)$$

and the creation operators are given by

$$\pi_{AW}^\beta(a_\lambda^*(f_\lambda)) = a_\lambda^*(\sqrt{1 + \rho_\beta} f_\lambda) \otimes \hat{1} + \hat{1} \otimes a_\lambda(\sqrt{\rho_\beta} \bar{f}_\lambda). \tag{27}$$

The function ρ_β is a physical input which ensures that Planck's law for the thermal radiation density and Bose–Einstein statistics is satisfied and we have

$$\rho_\beta(\vec{k}) = \frac{1}{e^{\beta\omega(\vec{k})} - 1}. \tag{28}$$

The vector representative Ω_{AW}^β of ω_{EM}^β is cyclic and separating for the weak closure $\pi_{AW}^\beta(\mathfrak{A}_{EM})''$ of \mathfrak{A}_{EM} and it turns out that $(\pi_{AW}^\beta(\mathfrak{A}_{EM})'', \{\pi_{AW}^\beta \circ \tau_t^{EM}\}_{t \in \mathbb{R}})$ is a W^* -dynamical system [42]. Using $(\mathfrak{H}_{AW}, \pi_{AW}^\beta)$ it can be derived that

$$\begin{aligned} \omega_{EM}^\beta(\tau_{z_2}^{EM}(\Phi(b_\varphi^\alpha(\vec{x})))) \tau_{z_1}^{EM}(\Phi(b_\varphi^\gamma(\vec{y}))) &= \frac{1}{2} \sum_{\lambda=1,2} \int_{\mathbb{R}^3} d^3k (\overline{b_{\varphi\lambda}^{\alpha(\vec{x},z_2)}(\vec{k})} b_{\varphi\lambda}^{\gamma(\vec{y},z_1)}(\vec{k}) (1 + \rho_\beta(\vec{k})) \\ &+ \overline{b_{\varphi\lambda}^{\gamma(\vec{y},z_1)}(\vec{k})} b_{\varphi\lambda}^{\alpha(\vec{x},z_2)}(\vec{k}) \rho_\beta(\vec{k})). \end{aligned} \tag{29}$$

For later purpose we define the *magnetic quantum exchange* $\mathfrak{m}_{\varphi\beta}^{\alpha\gamma}: \mathbb{R}^3 \times Z \times \mathbb{R}^3 \times Z \times \mathbb{R}^3 \rightarrow \mathbb{C}$ with the strip $Z = [0, \infty) \times [0, i\beta)$ in the complex plane \mathbb{C} by

$$\begin{aligned} (\vec{x}, z_2, \vec{y}, z_1, \vec{k}) \mapsto \mathfrak{m}_{\varphi\beta}^{\alpha\gamma}(\vec{x}, z_2, \vec{y}, z_1, \vec{k}) &\doteq \frac{1}{2} \sum_{\lambda=1,2} (\overline{b_{\varphi\lambda}^{\alpha(\vec{x},z_2)}(\vec{k})} b_{\varphi\lambda}^{\gamma(\vec{y},z_1)}(\vec{k}) (1 + \rho_\beta(\vec{k})) + \overline{b_{\varphi\lambda}^{\gamma(\vec{y},z_1)}(\vec{k})} b_{\varphi\lambda}^{\alpha(\vec{x},z_2)}(\vec{k}) \rho_\beta(\vec{k}) \\ &+ \overline{b_{\varphi\lambda}^{\gamma(\vec{y},z_2)}(\vec{k})} b_{\varphi\lambda}^{\alpha(\vec{x},z_1)}(\vec{k}) (1 + \rho_\beta(\vec{k})) + \overline{b_{\varphi\lambda}^{\alpha(\vec{x},z_1)}(\vec{k})} b_{\varphi\lambda}^{\gamma(\vec{y},z_2)}(\vec{k}) \rho_\beta(\vec{k})). \end{aligned} \tag{30}$$

The following useful symmetry is valid: $\mathfrak{m}_{\varphi\beta}^{\alpha\gamma}(\vec{x}, z_2, \vec{y}, z_1, \vec{k}) = \mathfrak{m}_{\varphi\beta}^{\alpha\gamma}(\vec{x}, z_1, \vec{y}, z_2, \vec{k})$. In applications to NMR it turns out that the family $\{\mathfrak{m}_{\varphi\beta}^{\alpha\gamma}\}_{\alpha,\gamma=x,y,z}$ takes a central role for the strength and occurrence of the magnetic shielding (chemical shift) and determines return to equilibrium properties.

4. Quantum spin systems and spin boson systems

In the perturbation series used in this document Quantum Spin Systems (QSS) occur as subsystems of Spin Boson Systems (SBS) while SBS occur as subsystems of the mQED systems.

Quantum Spin Systems. The mathematical framework for QSS is taken from [47, 59]. A quantum spin system consists of particles on a lattice \mathbb{Z}^d . We associate with each point $x \in \mathbb{Z}^d$ a Hilbert space \mathfrak{H}_x of dimension $2s(x) + 1$ and with a finite subset $\lambda = \{x_1, \dots, x_\nu\} \subset \mathbb{Z}^d$ we associate the tensor product space $\mathfrak{H}_\lambda = \bigotimes_{x_i \in \lambda} \mathfrak{H}_{x_i}$. The

lattice can be equipped with a metric $d(\cdot, \cdot)$. The local physical observables are contained in the algebra of all bounded operators acting on \mathfrak{H}_λ , that is the local C^* -algebra $\mathfrak{A}_\lambda \cong \bigotimes_{x_i \in \lambda} M_{2s(x_i)+1}$ in which M_n denote the algebra

of $n \times n$ complex matrices. If $\Lambda_1 \cap \Lambda_2 = \emptyset$, then $\mathfrak{H}_{\Lambda_1 \cup \Lambda_2} = \mathfrak{H}_{\Lambda_1} \otimes \mathfrak{H}_{\Lambda_2}$ and \mathfrak{A}_{Λ_1} is isomorphic to the C^* -subalgebra $\mathfrak{A}_{\Lambda_1} \otimes \hat{1}_{\Lambda_2}$ of $\mathfrak{A}_{\Lambda_1 \cup \Lambda_2}$, where $\hat{1}_{\Lambda_2}$ denotes the identity operator on \mathfrak{H}_{Λ_2} . If $\Lambda_1 \subseteq \Lambda_2$ then $\mathfrak{A}_{\Lambda_1} \subseteq \mathfrak{A}_{\Lambda_2}$ and operators with disjoint support commute, i.e. $[\mathfrak{A}_{\Lambda_1}, \mathfrak{A}_{\Lambda_2}] = 0$ whenever $\Lambda_1 \cap \Lambda_2 = \emptyset$. We may define the algebra of "all local observables" as $\mathfrak{A}_{loc} = \bigcup_{\Lambda \subset \mathbb{Z}^d} \mathfrak{A}_\Lambda$. The operator norm of an element $A \in \mathfrak{A}_\Lambda$ is given by

$\|A\| = \sup \{ \|A\Psi\|; \Psi \in \mathfrak{H}_\Lambda, \|\Psi\| = 1 \}$. An interaction Φ is defined to be a function from a finite subset $X \subset \mathbb{Z}^d$ into the hermitian elements of \mathfrak{A} such that $\Phi(X) \in \mathfrak{A}_X$. The Hamiltonian associated with the region Λ is then given by

$$H_\Phi(\Lambda) = \sum_{X \subseteq \Lambda} \Phi(X). \tag{31}$$

An interaction of a spin with a classical, external magnetic field [36, 60–62] is given by

$$\Phi(\{j\}) = \gamma_j \vec{I}_j \cdot \vec{B}_{ext} \quad \text{for nuclear spins and} \quad \Phi(\{i\}) = g_S \frac{\mu_B}{\hbar} \vec{S}_i \cdot \vec{B}_{ext} \quad \text{for spins of electrons.} \tag{32}$$

An NMR pulse induces a time-dependent interaction P_t involving spins and oscillating, external magnetic fields [63, 64]

$$P_t \doteq \sum_{j=1}^K \Phi_t^P(\{j\}), \quad \text{where} \quad \Phi_t^P(\{j\}) = \gamma_j \vec{I}_j \cdot \vec{B}_{ext}(t). \tag{33}$$

For example, a single pulse in x-direction, which is switched on from time $t = 0$ to $t = t_0$, is described by a magnetic field of the form

$$B_{\text{ext}}^y(t) = B_p \int d\omega_p f(\omega_p) \theta(t, 0, t_0) \cos(\omega_p t + \phi). \tag{34}$$

θ is the step function, B_p provides the amplitude of the pulse (some milli Tesla), ϕ is the phase of the magnetic field at $t = 0$ and f provides the frequency distribution of the pulse. Often, the frequency distribution provided by f is of rectangular form and of course it has to cover the excitation frequencies of the nuclei which shall be excited. The dynamical evolution of an observable $A \in \mathfrak{A}_\Lambda$ for a system with time-independent Hamiltonian $H_\Phi(\Lambda) \in \mathfrak{A}_\Lambda$ can be described by the Heisenberg relations

$$\tau_t^{S\Lambda}: \mathfrak{A}_\Lambda \rightarrow \mathfrak{A}_\Lambda, \quad A \mapsto \tau_t^{S\Lambda}(A) = e^{\frac{iH_\Phi(\Lambda)t}{\hbar}} A e^{-\frac{iH_\Phi(\Lambda)t}{\hbar}}. \tag{35}$$

Thus the map $t \in \mathbb{R} \mapsto \tau_t^{S\Lambda}$ is a one-parameter group of $*$ -automorphisms of the matrix algebra \mathfrak{A}_Λ and S denotes that this automorphism group acts only on the quantum spin algebra. The corresponding derivation is denoted by δ_Λ and $(\mathfrak{A}_\Lambda, \tau_t^{S\Lambda})$ is a C^* -dynamical system because $\tau_t^{S\Lambda}$ is strongly continuous for finite external fields. Since effective spin-spin couplings are absent in the mQED Hamiltonian equation (5) and (6) a spin system consisting of K nuclei and E electrons forms a subsystem of (5) whose equilibrium state is given by

$$\omega_S^\beta = \bigotimes_{j=1}^{K+E} \omega_{S_j}^\beta. \tag{36}$$

$\omega_{S_j}^\beta$ is the (τ^{S_j}, β) -KMS state of the single nucleus or electron enumerated by j . The representation which is induced by ω_S^β is denoted by (\mathfrak{H}_S, π_S) .

Perturbative description of Spin Boson Systems. A C^* -algebra \mathfrak{A}_{SB} for spins located in Λ interacting with bosons from the quantized electromagnetic field is given by

$$\mathfrak{A}_{\text{SB}} \doteq \overline{\text{span}\{A \otimes W(f) | A \in \mathfrak{A}_\Lambda, f \in \mathfrak{H}^\Gamma\}}^{\|\cdot\|_{\mathfrak{B}(\mathfrak{H}_{\text{SB}})}} = \mathfrak{A}_\Lambda \otimes \mathfrak{A}_{\text{EM}}, \tag{37}$$

where $\mathfrak{H}_{\text{SB}} = \mathfrak{H}_\Lambda \otimes \mathfrak{H}_{\text{AW}}^\Gamma$ is a representation space. The index Λ is neglected for simplicity. The free time evolution $\tau_t^{\text{SB}} = \tau_t^{S\Lambda} \otimes \tau_t^{\text{EM}}$, with derivation $\delta_{\text{SB}} = \delta_\Lambda + \delta_{\text{EM}}$, acts on \mathfrak{A}_{SB} and we have $\tau_t^{\text{SB}}(A \otimes W(f)) \in \mathfrak{A}_{\text{SB}}$ [42]. Interactions of the form

$$H_{\text{Int}}^{\text{SB}} = \sum_{\alpha=x,y,z} \left(\sum_{j=1}^K \gamma_j I_j^\alpha \otimes \Phi(b_\varphi^{\alpha \bar{x}_j}) + \sum_{i=1}^E g_S \frac{\mu_B}{\hbar} S_i^\alpha \otimes \Phi(b_\varphi^{\alpha \bar{x}_i^\dagger}) \right) \tag{38}$$

enable energy exchange between spins and bosons. Note that, for the sake of simplicity, we do not state the dependence on spatial coordinates on the left-hand side of this equation. Interactions given by (38) are unbounded and if the derivation induced by $H_{\text{Int}}^{\text{SB}}$ is denoted by $\delta_{\text{SB}}^{\text{Int}}$ then the evolution group $\{\tau_t^{\text{ISB}}\}_{t \in \mathbb{R}}$ generated by $\delta_{\text{SB}}^{\text{Int}} = \delta_{\text{SB}}^{\text{f}} + \delta_{\text{SB}}^{\text{Int}}$ does not necessarily leaves \mathfrak{A}_{SB} invariant. However, if some general conditions are satisfied [42] $\tau_t^{\text{ISB}}(A)$ lies in the weak closure $\mathfrak{A}_{\text{SB}}''$, i.e. $\tau_t^{\text{ISB}}(\mathfrak{A}_{\text{SB}}) \subseteq \mathfrak{A}_{\text{SB}}''$. Furthermore, if the conditions from [42] are satisfied the convergence of the right hand side of

$$\tau_t^{\text{ISB}}(A) = \tau_t^{\text{SB}}(A) + \sum_{n \geq 1} i^n \int_0^t dt_1 \int_0^{t_1} dt_2 \cdots \int_0^{t_{n-1}} dt_n [\tau_{t_n}^{\text{SB}}(H_{\text{Int}}^{\text{SB}}), [\cdots [\tau_{t_1}^{\text{SB}}(H_{\text{Int}}^{\text{SB}}), \tau_t^{\text{SB}}(A)]]] \tag{39}$$

towards $\tau_t^{\text{ISB}}(A)$ holds strongly on vectors of the form $|\Omega\rangle = |\Omega_\Lambda\rangle \otimes |\Omega_0\rangle$ and observables of the form $A = I \otimes W(f)$, where $I \in \mathfrak{A}_\Lambda$ and $|\Omega_\Lambda\rangle \in \mathfrak{H}_\Lambda$. For a large class of coupling functions φ [42] the pair

$$(\pi_{\text{SB}}^\beta(\mathfrak{A}_{\text{SB}}''), \pi_{\text{SB}}^\beta \circ \tau^{\text{ISB}}) \tag{40}$$

is a W^* -dynamical system and $\pi_{\text{SB}}^\beta = \pi_S \otimes \pi_{\text{AW}}^\beta$. An important state $\hat{\omega}_{\text{SB}}^\beta$ on the von Neumann algebra $\pi_{\text{SB}}^\beta(\mathfrak{A}_{\text{SB}}'')$ is given by [47]

$$\hat{\omega}_{\text{SB}}^{\text{I}\beta}(A) = \hat{\omega}_{\text{SB}}^\beta(A) + \sum_{n \geq 1} (-1)^n \int_0^\beta ds_1 \int_0^{s_1} ds_2 \cdots \int_0^{s_{n-1}} ds_n \hat{\omega}_{\text{T,SB}}^\beta(A, \hat{\tau}_{is_n}^{\beta\text{SB}}(H_{\text{Int}}^{\text{SB}}), \dots, \hat{\tau}_{is_1}^{\beta\text{SB}}(H_{\text{Int}}^{\text{SB}})), \tag{41}$$

where $\hat{\omega}_{\text{SB}}^\beta$ is the extension of $\omega_{\text{SB}}^\beta = \omega_S^\beta \otimes \omega_{\text{EM}}^\beta$ on \mathfrak{A}_{SB} to $\pi_{\text{SB}}^\beta(\mathfrak{A}_{\text{SB}}'')$, $\hat{\tau}^{\beta\text{SB}} \doteq \pi_{\text{SB}}^\beta \circ \tau^{\text{SB}}$, $A \in \pi_{\text{SB}}^\beta(\mathfrak{A}_{\text{SB}}'')$ and T denotes that truncated functions are used [47]. If the conditions from [42] are satisfied one finds for a large class of states η and observables A return to equilibrium for the interacting system, formally given by

$$\lim_{t \rightarrow \infty} \eta \circ \tau_t^{\text{ISB}}(A) = \omega_{\text{SB}}^{\text{I}\beta}(A). \tag{42}$$

In this case $\omega_{\text{SB}}^{\text{I}\beta}$ is a $(\tau^{\text{ISB}}, \beta)$ -KMS state. For applications to NMR we define the evolution group $\{\tau_{P_t}^{\text{ISB}}\}_{t \in \mathbb{R}}$ which is generated by $\delta_{\text{SB}}^{\text{I}} + \delta_{P_t}$. For $A \in \mathfrak{A}_\Lambda$ we have $\delta_{P_t}(A) = i[P_t, A]$ and $t \in \mathbb{R} \mapsto P_t = P_t^* \in \mathfrak{A}_\Lambda$ is a one-parameter family of selfadjoint elements which contains the information of the pulse sequence given by equation (33). From now on we make the identification $\mathfrak{M} = \mathfrak{A}_{\text{SB}}''$. Although there exist not yet a rigorous proof it seems to be obvious [65] that if $(\pi_{\text{SB}}^\beta(\mathfrak{A}_{\text{SB}}''), \pi_{\text{SB}}^\beta \circ \tau^{\text{ISB}})$ is a W^* -dynamical system then $(\pi_{\text{SB}}^\beta(\mathfrak{M}), \pi_{\text{SB}}^\beta \circ \tau_P^{\text{ISB}})$ is a W^* -dynamical system for a suitable class of pulse sequences P .

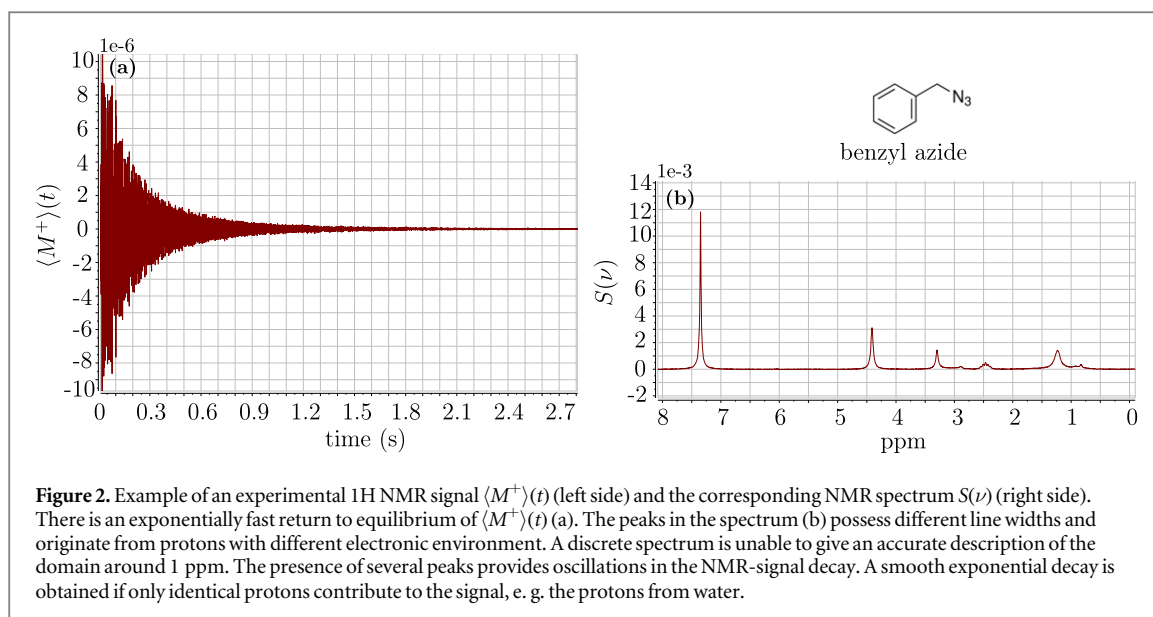


Figure 2. Example of an experimental ^1H NMR signal $\langle M^+ \rangle(t)$ (left side) and the corresponding NMR spectrum $S(\nu)$ (right side). There is an exponentially fast return to equilibrium of $\langle M^+ \rangle(t)$ (a). The peaks in the spectrum (b) possess different line widths and originate from protons with different electronic environment. A discrete spectrum is unable to give an accurate description of the domain around 1 ppm. The presence of several peaks provides oscillations in the NMR-signal decay. A smooth exponential decay is obtained if only identical protons contribute to the signal, e.g. the protons from water.

5. Application to NMR

A typical NMR experiment consists basically of molecules interacting with external magnetic fields. In most experiments the interacting system is in thermal equilibrium at the beginning of the experiment. The molecular structures are then investigated by the application of a pulse sequence which consists of oscillating, external magnetic fields. Pulse sequences provide an out of equilibrium nuclear spin dynamics and they act only for a short time at the beginning of the experiment. When the pulse sequence is finished the system is again governed by the equilibrium dynamics which is then responsible for a return to equilibrium. This equilibration process is experimentally detected in NMR and referred as *free induction decay* (FID). In most experiments the x- and y-components of the nuclear spins are recorded, while the z-component is not recorded. The detected FID is called NMR signal, $\langle M^+ \rangle(t)$, and its Fourier transform provides the NMR spectrum $S(\nu)$. An NMR spectrometer detects the radiation from the magnetically excited nuclear spins which is identical to the time evolution of the x- and y-components of the nuclear spins. Therefore, the NMR spectrometer records the NMR signal $\langle M^+ \rangle(t) = \sum_j \langle I_j^+(t) \rangle$ which consists of expectation values with observables $I_j^+(t) = I_j^x(t) + iI_j^y(t)$. The real and imaginary parts of the NMR signal are given by $\Re(\langle M^+ \rangle(t)) = \sum_j \langle I_j^x(t) \rangle$ and $\Im(\langle M^+ \rangle(t)) = \sum_j \langle I_j^y(t) \rangle$ respectively. In certain cases, the NMR spectrum contains only very sharp peaks of "Lorentzian shape". NMR spectra which show any other distribution may be obtained by (continuous) superpositions of Lorentz functions. It is usually seen that the positions of the peaks are shifted towards lower frequencies compared to the *Larmor frequency* $\nu_0 = \gamma|B_{\text{ext}}^z|$. This is called *chemical shift* and it is a direct consequence of the magnetic shielding which is caused by the electrons: In the presence of an external magnetic field the magnetic moments of electrons show into the opposite direction compared to the magnetic moments of the nuclei. Hence, the external magnetic field at the position of a nucleus is reduced (shielded) by electrons.

Figure 2 shows exemplary ^1H NMR-data of $12 \mu\text{l}$ benzyl azide with impurities in dimethyl sulfoxide- D_6 . The NMR signal $\langle M^+ \rangle(t)$ is shown in (a) and the spectrum $S(\nu)$ in (b). An exponentially fast thermalization for $\langle M^+ \rangle(t)$ can be seen on the left image. Note that this is the thermalization for the expectation values of x- and y-components of nuclear spin operators. The z-component needs an equal or more time for return to equilibrium. The Fourier transform (right image) provides the frequencies involved in the nuclear spin dynamics during thermalization. It can be seen that the peaks possess different widths and positions. The domain around 1 and 3 ppm is generated only by a few protons but the description of this domain by a discrete spectrum is not accurate. Hence, model-calculations involving a continuous spectrum are desirable for a detailed analysis of this spectrum. The different line widths contain important information about the distribution of the electrons and nuclei.

According to the description of an experimental NMR setup the mQED system in the algebraic framework is applied as follows. At times before pulse sequences, $t \leq 0$, the description of the molecular system interacting with the classical and quantized electromagnetic field will be described by the Hamiltonian $H = H_0 + H_{\text{Int}}^{\text{SB}}$ from equation (5) and (38). $H_{\text{Int}}^{\text{SB}}$ contains the same interactions as H_{Int} from equation (6) except the interactions which does not involve spins. Hence, it may be referred as Spin Boson approximation of mQED. This approximation is based on the assumption that the energy of a pulse sequence is too low to change the

momentum and geometry of the investigated electronic structure. This approximation is also made by the effective spin model and there seems to be no obvious reason why this approximation should be unsuitable. For $t = 0$ the system is in thermal equilibrium and the equilibrium state Ω^β is determined by H . Pulse sequences are initiated at $t = 0$, such that for $t > 0$ the system is described by $H + P_t$. The time-dependent operator P_t from equation (33) contains the information of the pulse sequence. Hence, the time-dependence of a nuclear spin operator, e.g., $I^-(t)$ or $I^+(t)$, during a pulse sequence is determined by $H + P_t$.

In the application to NMR the Born-Oppenheimer approximation will be used. The wave function ψ of the electrons will be approximated by the ground state but use a temperature dependent nuclear wave function Ψ^β . Hence, our molecular system is described by the wave function $\Psi^\beta \otimes \psi \in \mathfrak{H}_M$. Ideally the KMS state is used for the nuclei. However, in most cases it is practically not possible to estimate this KMS state explicitly. This is because the nuclear Schrödinger equation can only be solved for very simple molecules. Therefore, a suitable procedure may be used which approximates the square $|\Psi^\beta(X)|^2$ of the vector representative of the KMS state. A suitable initial choice may be given by inserting the potential energy surface (PSE) into the classical Gibbs state at inverse temperature β . If a $|\Psi^\beta(X)|^2$ is found which shows agreement between experimental and calculated NMR spectra then a suitable approximation for the probability distribution of the nuclei is obtained. Let $\mathfrak{B}(\mathfrak{H}_M)$ denote the set of bounded operators on the Hilbert space \mathfrak{H}_M of molecular systems. The spatial structure of the molecular system is contained in the state $\omega_M^\beta: \mathfrak{B}(\mathfrak{H}_M) \rightarrow \mathbb{C}$. For a function $f \in \mathfrak{B}(\mathfrak{H}_M)$ the expectation value is given by

$$\omega_M^\beta(f) = \int d^{3K}x \int d^{3E}x^e |\Psi^\beta(X)|^2 |\psi(X, X^e)|^2 f(X, X^e). \quad (43)$$

Remember that the dependence of $\tau_{P_t}^{ISB}$ and $\hat{\omega}_{SB}^{I\beta}$ on the coordinates (X, X^e) was so far neglected in the notation for simplicity. For the main result this dependence is now written explicitly for clarity. Usually the temperature dependence is not explicitly indicated for the NMR-signal but we will do this in the following.

Main Result (NMR-signal from mQED):

Assume that $(\mathfrak{M}, \tau_P^{ISB})$ is a W^* -dynamical system and that $\omega_{SB}^{I\beta}$ is a (τ_P^{ISB}, β) -KMS state. Furthermore, let

$$\tau_{P_t}^{ISB}: \mathfrak{M} \rightarrow \mathfrak{M}, \quad \pi_{SB}^\beta: \mathfrak{M} \rightarrow \mathfrak{B}(\mathfrak{H}_{SB}) \quad \text{and} \quad \hat{\omega}_{SB}^{I\beta}: \mathfrak{B}(\mathfrak{H}_{SB}) \rightarrow \mathbb{C} \quad (44)$$

be constructed as in section 4 and let $\mathfrak{L}_t^\beta: \mathfrak{A}_\Lambda \rightarrow \mathfrak{B}(\mathfrak{H}_M)$, $\mathfrak{A}_\Lambda \ni A \mapsto \mathfrak{L}_t^\beta(A) \in \mathfrak{B}(\mathfrak{H}_M)$ be given by

$$\mathfrak{L}_t^\beta(A): \mathbb{R}^{3K} \times \mathbb{R}^{3E} \rightarrow \mathbb{C} \quad \text{with} \quad \mathbb{R}^{3K} \times \mathbb{R}^{3E} \ni (X, X^e) \mapsto \mathfrak{L}_t^\beta(A)(X, X^e) \equiv \hat{\omega}_{SB}^{I\beta}(\pi_{SB}^\beta \circ \tau_{P_t}^{ISB}(A))(X, X^e). \quad (45)$$

We calculate $\hat{\omega}_{SB}^{I\beta}$ according to equation (41) and $\tau_{P_t}^{ISB}(A)$ according to equation (39), by using $H_{\text{Int}}^{SB} + P_t$ instead of H_{Int}^{SB} . For a molecular system described by ω_M^β according to equation (43) the NMR signal $\langle M^+ \rangle_\beta(t)$ is defined by

$$\langle M^+ \rangle_\beta(t) \doteq \sum_{j=1}^K \omega_M^\beta(\mathfrak{L}_t^\beta(I_j^+)). \quad (46)$$

A reconstruction of the probability density $|\Psi^\beta(X)|^2$ for the spatial distribution of the nuclei is achieved by identifying an ω_M^β which provides a sufficient agreement between the calculated and the experimental NMR spectrum.

An identification of ω_M^β may initially be based on approximations for the nuclear wave function as described in [13] or by inserting the PES into the classical Gibbs state with subsequent manual adaptations until the calculated spectrum shows sufficient agreement with the experimental spectrum. Note that \mathfrak{L}_0^β gives thermal equilibrium at the beginning of the experiment and $\mathfrak{L}_{t>0}^\beta$ describes the time-evolution during the experiment. The notation $\mathfrak{L}_t^\beta(A)(X, X^e)$ is unconventional but easier to read in later applications. A conventional notation is given by $\mathfrak{L}_{\beta t}^A(X, X^e) \equiv \mathfrak{L}_t^\beta(A)(X, X^e)$ but this is more difficult to read when dealing with $\omega_M^\beta(\mathfrak{L}_{\beta t}^A)$. As usual the (1-dimensional) NMR spectrum, $S_\beta(\nu)$, is calculated as the Fourier transform

$$S_\beta(\nu) = \int_0^\infty dt \langle M^+ \rangle_\beta(t) e^{-i\nu t}. \quad (47)$$

The structural validity of the main result will now be checked in the next two sections.

6. Breakdown of the effective spin model

The breakdown of the effective spin model is shown for the time-independent expectation value in thermal equilibrium as well as for the out of equilibrium spin dynamics. One observes that the mQED perturbation series contains several terms which have a similar structure as individual interactions contained in the effective spin model equation (1). For example, it is possible to extract terms of the form $J_{ij}^{zz} I_i^z \otimes I_j^z$ from the mQED perturbation series (see equation (55)) and J_{ij}^{zz} contains probabilities for the propagation of magnetic field quanta between the spins. Analogous terms for magnetic shielding can also be found (see equation (49)). Hence,

the effective spin model is in some sense contained in the mQED model but with quantum radiative corrections and other types of corrections. Of course, the mQED model is *not* an effective description since all interactions are naturally generated by the fundamental theory of mQED. This is investigated in more detail in this section. Details of the calculations are shifted to the [appendix](#).

In thermal equilibrium the expectation value of the z-component of a nuclear spin of a molecule is reduced, if compared to the case where the spin is isolated. This is due to the action of the external magnetic field on the magnetic moments of the surrounding electrons, which then reduce the external magnetic field at the positions of the nuclei. For diagonal σ_j the effective model from equation (1) provides

$$\langle I_j^z \rangle_{\text{eff}} = \text{Tr}(\rho_{\text{eff}}^\beta I_j^z) \approx \frac{\hbar^2}{4} \beta \gamma_j B_{\text{ext}}^z (1 - \sigma_j^{zz}) \quad \text{where} \quad \rho_{\text{eff}}^\beta = \frac{\exp(-\beta H_{\text{eff}})}{\text{Tr}(\exp(-\beta H_{\text{eff}}))}. \quad (48)$$

Higher order terms can be neglected in the high temperature approximation. The effective magnetic shielding (chemical shift) constant is always small and positive, i. e., $1 \gg \sigma_j^{zz} > 0$. Hence, the expectation value of an isolated nuclear spin is reduced in the molecular system by σ_j^{zz} .

In this document the hydrogen atom is used as basic example for mQED calculations. One finds similar results for a Helium atom and a discussion on that can be found in the [appendix](#). Remember that I^z denotes the z-component of the spin operator of the proton while S^z denotes the operator from the electron. While the first order of equation (41) is zero for $A = I^z$ one derives in the zeroth and second order that (details are given in the [appendix](#))

$$\omega_M^\beta(\Omega_0^\beta(I^z)) = \omega_S^\beta(I^z) - \omega_S^\beta(S^z) r_\varphi^\beta + \dots \quad (49)$$

$$\approx \frac{\hbar^2}{4} \beta \gamma B_{\text{ext}}^z (1 - a_\varphi^\beta). \quad (50)$$

The dots (...) denote higher order terms from the perturbation series. r_φ^β and a_φ^β differ by a constant and the high temperature approximation is made for $\omega_S^\beta(I^z)$ and $\omega_S^\beta(S^z)$. It can be seen that a_φ^β , derived *non-effectively* from mQED, replaces the effective parameter σ_j^{zz} which is commonly derived according to equation (2). This is easily verified by comparing equation (48) with (49) and a more detailed discussion of this can be found in the [appendix](#). It can be checked that a_φ^β is dimensionless and therefore a_φ^β can be given in "parts per million" (ppm) in analogy to σ^{zz} . One finds

$$a_\varphi^\beta = \frac{g_s^2 \mu_B^2}{4} \int_0^{\beta} ds_1 \int_0^{s_1} ds_2 \iiint_{\mathbb{R}^3} d^3x \iiint_{\mathbb{R}^3} d^3x^e \iiint_{\mathbb{R}^3} d^3k |\Psi^\beta(\vec{x})|^2 |\psi_{100}(\vec{x}, \vec{x}^e)|^2 m_{\varphi\beta}^{zz}(\vec{x}, is_2, \vec{x}^e, is_1, \vec{k}). \quad (51)$$

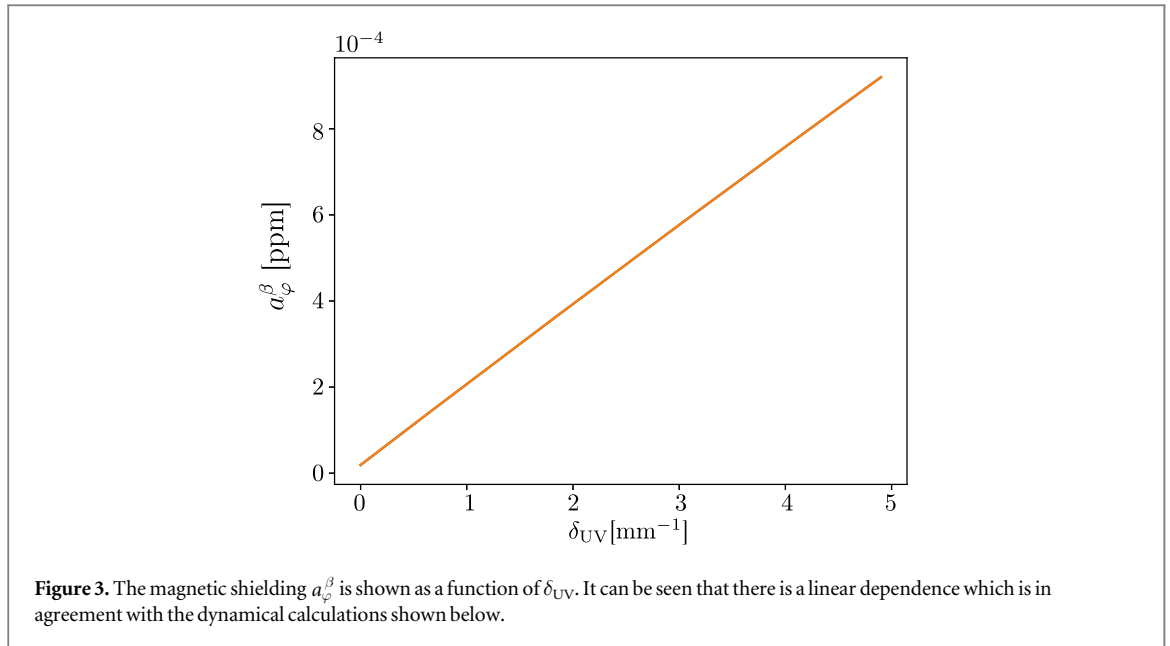
In case of a hydrogen atom a_φ^β is indeed independent from a particular choice of the nuclear wave function Ψ^β . This reflects the fact that the magnetic shielding is independent from the position of the atom in the homogeneous external field. The distribution of the electron is chosen to be the 1-s orbital of the hydrogen atom, i. e.

$$\psi_{100}(\vec{x}, \vec{x}^e) = \frac{1}{\sqrt{\pi a_B^3}} \exp\left(\frac{-|\vec{x} - \vec{x}^e|}{a_B}\right), \quad (52)$$

where a_B is the Bohr radius.

Observation 1

A comparison provides a further advantage for the non-effective model. For $B_{\text{ext}}^z \rightarrow \infty$ we have $\sigma^{zz} B_{\text{ext}}^z \rightarrow \infty$. Hence, the effective model predicts that the magnetic field which originates from the electron and reduces the magnetic field at the position of the proton tends to infinity. This is certainly wrong because there is a maximum magnetic field strength which can be produced by the electron and the maximum is achieved when the spin of the electrons is completely in the $|+1/2\rangle$ or $|-1/2\rangle$ state. In contrast the mQED model contains this effect and the limit is given by $\text{Tr}(\rho_2^\beta S^z) \leq \hbar/2$ in equation (49). In this case the high temperature approximation made in a_φ^β is unsuitable and equation (49) provides more accurate predictions than equation (50). Thus, for low temperatures and high external magnetic fields the mQED model is much more realistic. The deviation from the non-linear regime for $\sigma^{zz} B_{\text{ext}}^z \rightarrow \infty$ may be measured experimentally and validates the more realistic description of the mQED model. This is of potential relevance for NMR at low temperatures, e. g. Dynamic Nuclear Polarization (DNP).



Observation 2

We have $a_\varphi^\beta > 0$ for all $\varphi \in L^2(\mathbb{R}^3)$ which follows from the fact that φ enters a_φ^β with $|\varphi(\vec{k})|^2$ and

$$a_\varphi^\beta = \frac{g_s^2 \mu_B^2 \mu_0}{6\pi^2 \hbar c} \int_0^\infty dk |\varphi(k)|^2 \underbrace{\left(\frac{e^{-2\beta \hbar c k}}{2} - e^{-\beta \hbar c k} + 0.5 \right)}_{>0 \forall k \in \mathbb{R}^+} (1 + 2\rho^\beta(k)) \frac{k}{(1 + k^2 a_B^2/4)^2}. \quad (53)$$

In equation (53) spherical coordinates were introduced for \vec{k} and all integrals except the one for k were evaluated. Furthermore, we have assumed that φ depends only on $|\vec{k}|$ which is a natural and common choice. This is a nice result, because the non-effective magnetic shielding a_φ^β needs to be positive in any case and φ is a free parameter in mQED.

Numerical investigation of a_φ^β .

It is important to know that for any given molecular structure the coupling function φ from equation (10) is the only free parameters and—of course— φ is independent of Ψ and ψ . Thus, a particular choice for φ which accurately reproduces a well-understood experiment can be used to predict or analyze NMR data of proposed or unknown molecular structures. We have $g_s^2 \mu_B^2 \mu_0 / 6\pi^2 \hbar c \approx 7.271\,326\,950\,237\,399 \cdot 10^{-8} \text{ \AA}^2$, where \AA is the unit Ångström. For the numerical calculations we choose

$$\varphi(k) = \begin{cases} g & \text{for } \delta_{IR} \leq k \leq \delta_{UV} \\ 0 & \text{for } k < \delta_{IR} \vee k > \delta_{UV} \end{cases} \quad g, \delta_{UV} \in \mathbb{R}^+ \quad \text{and} \quad \delta_{UV} > \delta_{IR} \in \mathbb{R}_0^+. \quad (54)$$

δ_{IR} and δ_{UV} are the infrared and ultraviolet cutoff respectively and normalization of φ implies $g = 1/(\delta_{UV} - \delta_{IR})$. For the numerical calculations in this document the infrared cutoff δ_{IR} can be chosen arbitrarily small (and also zero) such that it has a negligible influence on a_φ^β .

Figure 3 shows the dependence of a_φ^β on δ_{UV} for a hydrogen atom. The unit of δ_{UV} is millimeter⁻¹ ($1 \text{ mm}^{-1} \approx 0.001\,24 \text{ eV}$). The temperature is chosen to be $T = 293 \text{ K}$ (room temperature) and the infrared cutoff is chosen to be zero, $\delta_{IR} = 0$. There is a linear increase of a_φ^β for increasing δ_{UV} which is in agreement with the dynamical calculations shown below. The ppm (parts per million) scale is chosen such that the Larmor frequency ν_0 is located at zero. Higher order contributions should increase the magnetic shielding.

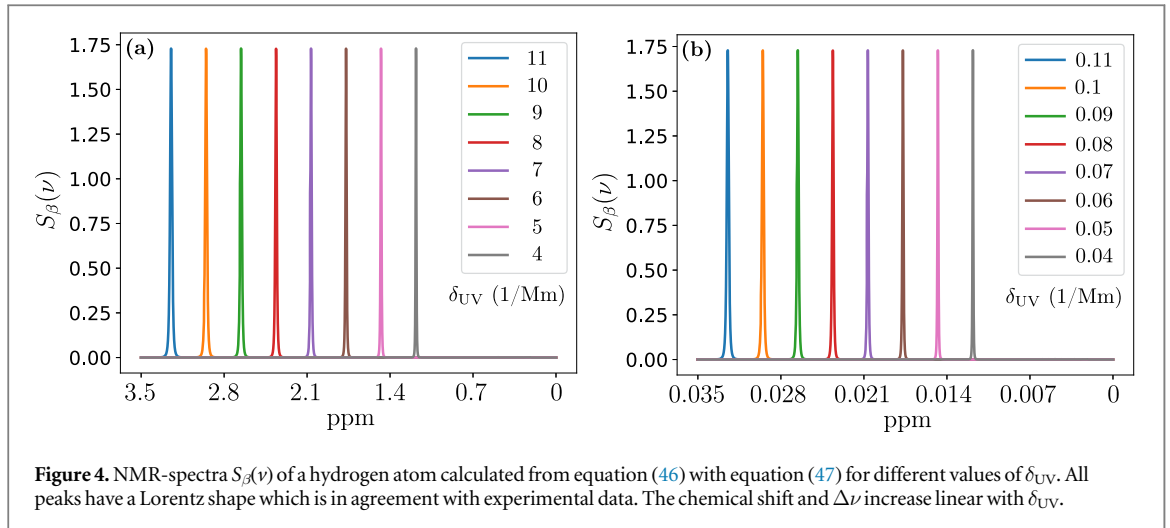
The dynamic case. Analytically the breakdown of the effective model can, for example, be seen by the occurrence of direct spin-spin interactions (dipole-dipole interactions) in the second order of equation (39). One finds,

$$[\tau_{t_2}^{SB}(H_{Int}^{SB}), [\tau_{t_1}^{SB}(H_{Int}^{SB}), \tau_{t_1}^{SB}(I^+)]] = \sum_{i < j} J_{ji}^{zz}(t, t_1, t_2) I_j^z \otimes I_i^z + \dots \quad (55)$$

with

$$J_{ji}^{zz}(t, t_1, t_2) = -\gamma_j \gamma_i u_j(t) \bar{u}_j(t_1) ([B_{0\varphi}^z(\vec{x}_i, t_2), B_{0\varphi}^x(\vec{x}_j, t_1)] + i[B_{0\varphi}^z(\vec{x}_i, t_2), B_{0\varphi}^y(\vec{x}_j, t_1)]). \quad (56)$$

and similar terms for the x- and y-components. Following the calculations from [66] the direct coupling $\vec{I}_i D_{ij} \vec{I}_j$ from the effective model equation (1) is obtained with quantum radiative corrections. Indirect spin-spin



couplings occur in the fourth order of equation (39) in a similar fashion. For the magnetic shielding in the dynamic case the numerical investigation of the breakup of the effective spin model is detailed shown in the next section.

7. NMR spectra from molecular Quantum Electrodynamics at finite temperatures

The real-time nuclear spin dynamics as well as the spectra according to equation (47) are calculated in the second order of equation (39) and the second order of equation (41) according to equation (46) and equation (47). After long-lasting calculations NMR-spectra are obtained from terms of the form

$$\begin{aligned}
 S_\beta(\nu) = & \vartheta_1 \int_0^\infty dt e^{-i\nu t} \int_0^\beta ds_1 \int_0^{s_1} ds_2 \int_0^t dt_1 \int_0^{t_1} dt_2 \iiint_{\mathbb{R}^3} d^3x \iiint_{\mathbb{R}^3} d^3x^e \iiint_{\mathbb{R}^3} d^3k \iiint_{\mathbb{R}^3} d^3k' \times \\
 & \times |\Psi^\beta(\vec{x})|^2 |\psi_{100}(\vec{x}, \vec{x}^e)|^2 \times \\
 & \times (\mathbf{m}_{\varphi\beta}^{xz}(\vec{x}, is_2, \vec{x}^e, is_1, \vec{k}') \omega_S^\beta(I^Y \tau_{is_2}(I^X)) + \mathbf{m}_{\varphi\beta}^{yz}(\vec{x}, is_2, \vec{x}^e, is_1, \vec{k}') \omega_S^\beta(I^Y \tau_{is_2}(I^Y))) \times \\
 & \times \sum_{\lambda=1,2} \varphi_\lambda^z(\vec{k}) (\varphi_\lambda^x(\vec{k}) + i\varphi_\lambda^y(\vec{k})) i\Delta_{\vec{k}}(\vec{x}^e, t_2) - (\vec{x}, t_1) u(t) \bar{u}(t) + \dots
 \end{aligned} \quad (57)$$

where $u(t) = e^{-it\nu_0}$ and $\vartheta_1 \in \mathbb{C}$. In case of the hydrogen atom one finds again that $S_\beta(\nu)$ is independent of Ψ^β which means that the chemical shift does not depend on the position of the hydrogen atom in the homogenous external field. For molecules with two or more nuclei $S_\beta(\nu)$ depends on Ψ^β and a discussion on the computational efforts for complex molecules is given in the [appendix](#).

Figure 4 shows the NMR spectra $S_\beta(\nu)$ from equation (46) with equation (47) for a hydrogen atom. The ppm scale is chosen such that the Larmor frequency ν_0 is located at zero ppm. The spectra is calculated for the values $\delta_{UV} = 4, 5, 6, 7, 8, 9, 10, 11$ (a) and $\delta_{UV} = 0.04, 0.05, 0.06, 0.07, 0.08, 0.09, 0.01, 0.011$ with unit megameter⁻¹ (Mm^{-1}). The temperature is chosen to be $T = 293$ K (room temperature), $B_{\text{ext}}^z = 20$ T (Tesla) and the infrared cutoff is chosen to be zero, $\delta_{\text{IR}} = 0$. In every case it can be seen that a Lorentz distribution is obtained as observed in NMR experiments. Small variations of δ_{IR} only had a negligible impact on the magnetic shielding. As in the case for a_φ^β the strength of the magnetic shielding increases linear with δ_{UV} . Furthermore, the "Full Width at Half Maximum" (FWHM) $\Delta\nu$ increases linearly with increasing δ_{UV} . Remember that $\Delta\nu$ is directly related with the life-time of an excited spin which will be checked later. Comparing the left figure (a) and the right figure (b) one finds that if δ_{UV} is reduced by a factor of 100 then $\Delta\nu$ as well as strength of the magnetic shielding (distance of the peak to 0 ppm) is also reduced by a factor of 100. The maximum value (height) of each peak is nearly the same. This a result of the normalization of φ and it makes sense because these small changes of the magnetic field strength should not have a significant impact on the amplitude of the NMR signal. This is also in agreement with experimental data.

Figure 5(a) shows the long-time dynamics of $\langle I^x \rangle(t)$ (real part of NMR-signal) for $\delta_{UV} = 0.1$ Mm (orange line) and $\delta_{UV} = 0.05$ Mm (blue line). All other parameters are the same as for the calculations for figure 4. In both cases there is an exponentially fast return to equilibrium as observed in NMR experiments. The starting point at $t = 0$ is chosen to be directly after the 90°-pulse has finished. The amplitudes are normalized to the value 0.5 at $t = 0$ corresponding to the excitation of a single nucleus. The thermalization which is associated with the orange line happens twice as fast as the thermalization which is associated with the blue line. Hence, doubling the

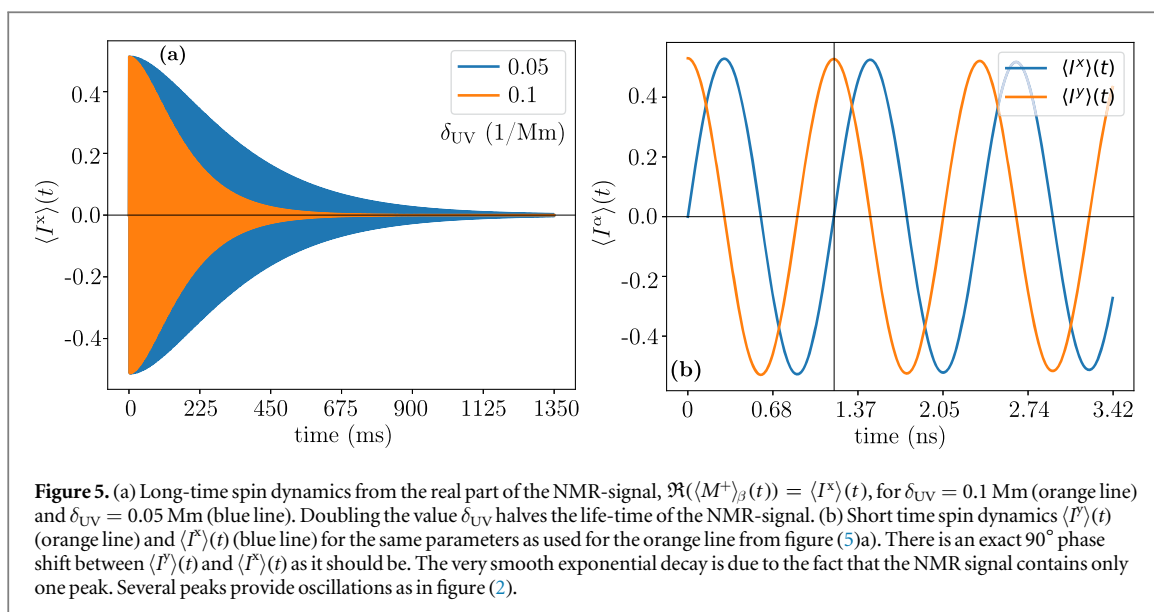


Figure 5. (a) Long-time spin dynamics from the real part of the NMR-signal, $\Re(\langle M^+ \rangle_\beta(t)) = \langle I^x \rangle(t)$, for $\delta_{UV} = 0.1$ Mm (orange line) and $\delta_{UV} = 0.05$ Mm (blue line). Doubling the value δ_{UV} halves the life-time of the NMR-signal. (b) Short time spin dynamics $\langle I^y \rangle(t)$ (orange line) and $\langle I^x \rangle(t)$ (blue line) for the same parameters as used for the orange line from figure 5(a). There is an exact 90° phase shift between $\langle I^y \rangle(t)$ and $\langle I^x \rangle(t)$ as it should be. The very smooth exponential decay is due to the fact that the NMR signal contains only one peak. Several peaks provide oscillations as in figure (2).

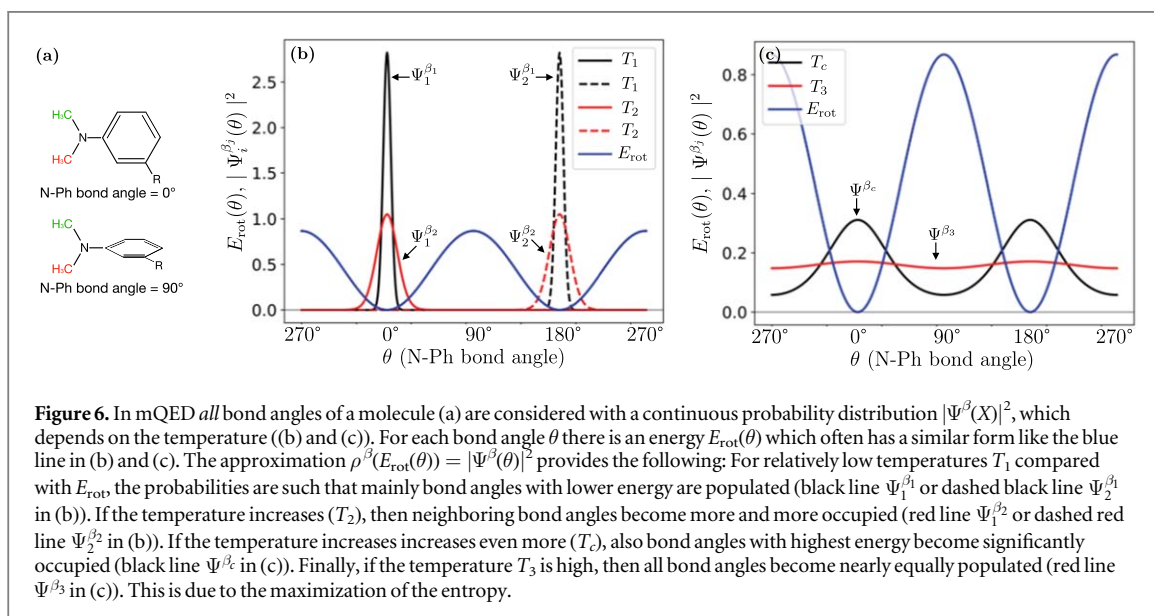


Figure 6. In mQED all bond angles of a molecule (a) are considered with a continuous probability distribution $|\Psi^\beta(X)|^2$, which depends on the temperature (b) and (c). For each bond angle θ there is an energy $E_{rot}(\theta)$ which often has a similar form like the blue line in (b) and (c). The approximation $\rho^\beta(E_{rot}(\theta)) = |\Psi^\beta(\theta)|^2$ provides the following: For relatively low temperatures T_1 compared with E_{rot} , the probabilities are such that mainly bond angles with lower energy are populated (black line $\Psi_1^{\beta_1}$ or dashed black line $\Psi_2^{\beta_1}$ in (b)). If the temperature increases (T_2), then neighboring bond angles become more and more occupied (red line $\Psi_1^{\beta_2}$ or dashed red line $\Psi_2^{\beta_2}$ in (b)). If the temperature increases even more (T_c), also bond angles with highest energy become significantly occupied (black line Ψ^{β_c} in (c)). Finally, if the temperature T_3 is high, then all bond angles become nearly equally populated (red line Ψ^{β_3} in (c)). This is due to the maximization of the entropy.

value δ_{UV} halves the life-time (T2 in NMR language) of the excited spin. The nuclear spin can release energy in a frequency range with double length.

Figure 5(b) shows the short-time dynamics $\langle I^y \rangle(t) = \Im(\langle M^+ \rangle_\beta(t))$ and $\langle I^x \rangle(t) = \Re(\langle M^+ \rangle_\beta(t))$ for the same parameters which were used for the orange line from figure 5(a). The cross shows that there is an exact 90° phase shift between $\langle I^y \rangle(t)$ and $\langle I^x \rangle(t)$ as it should be. The frequency is slightly reduced compared to the Larmor frequency which can also be seen from figure 4(b).

8. Outlook

In this section it is outlined how the new approach can serve for a more detailed molecular structure determination compared to conventional NMR theory. To obtain an approximated amplitude square $|\Psi^\beta(X)|^2$ of the nuclear KMS state, the potential energy surface (PES), $E_{PES}(X)$, or rotational energies, $E_{rot}(\theta)$, from Quantum Chemistry may be inserted in to the classical Gibbs state ρ^β at inverse temperature β (figure 6).

From Quantum Statistical Mechanics we know that for different temperatures $T_1 < T_2 < T_c < T_3$ there are different probabilities $|\Psi^\beta(\theta)|^2$ for the molecule to have a certain bond angle θ (figure 6). Such effects can be observed in NMR, because the green and the red methyl groups (a) can have different electronic environments which depends on the temperature. The probability $|\Psi^\beta(\theta)|^2$ is time-independent in chemical and thermodynamic equilibrium such that the molecule is in a superposition of several bond angles. This is in

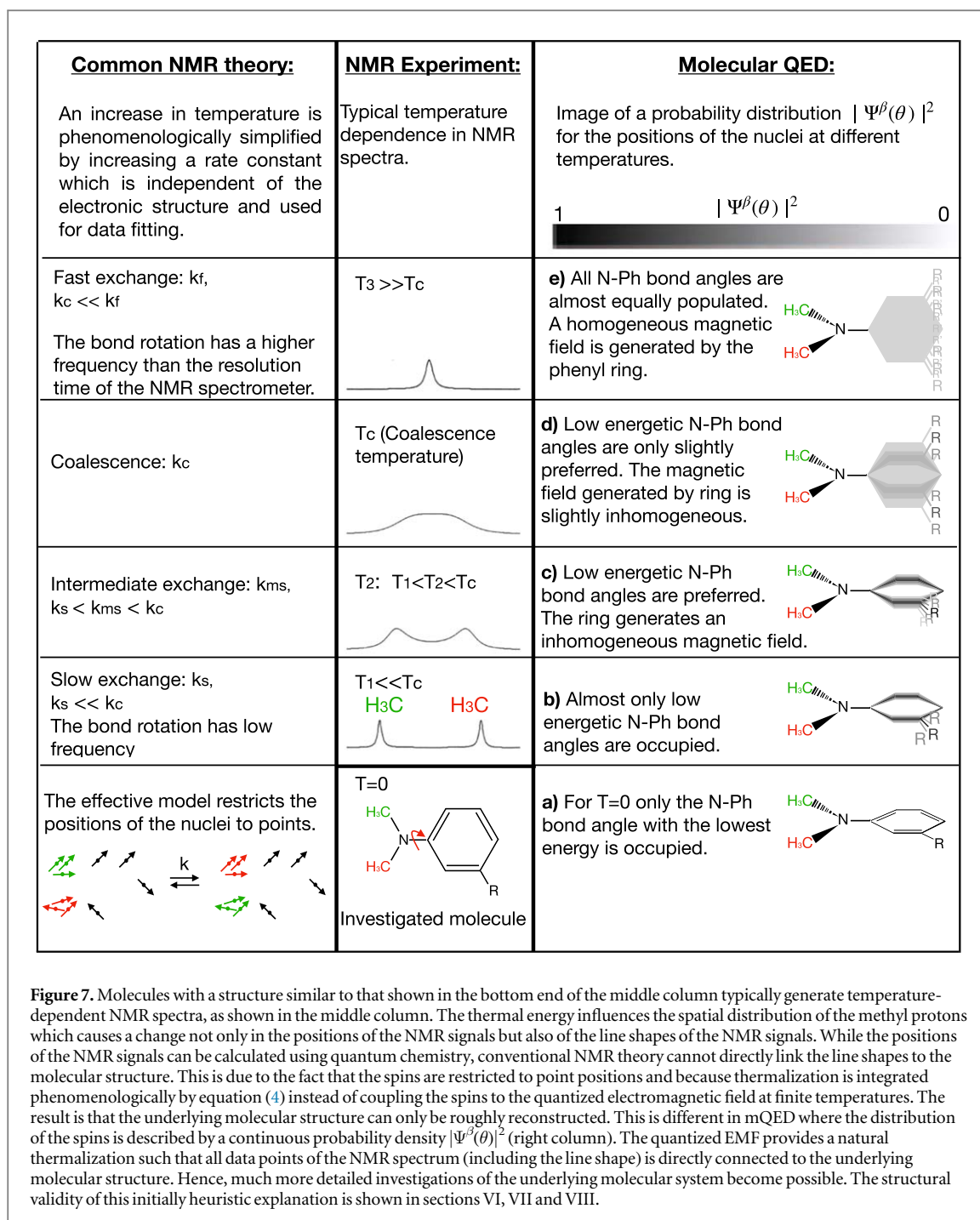
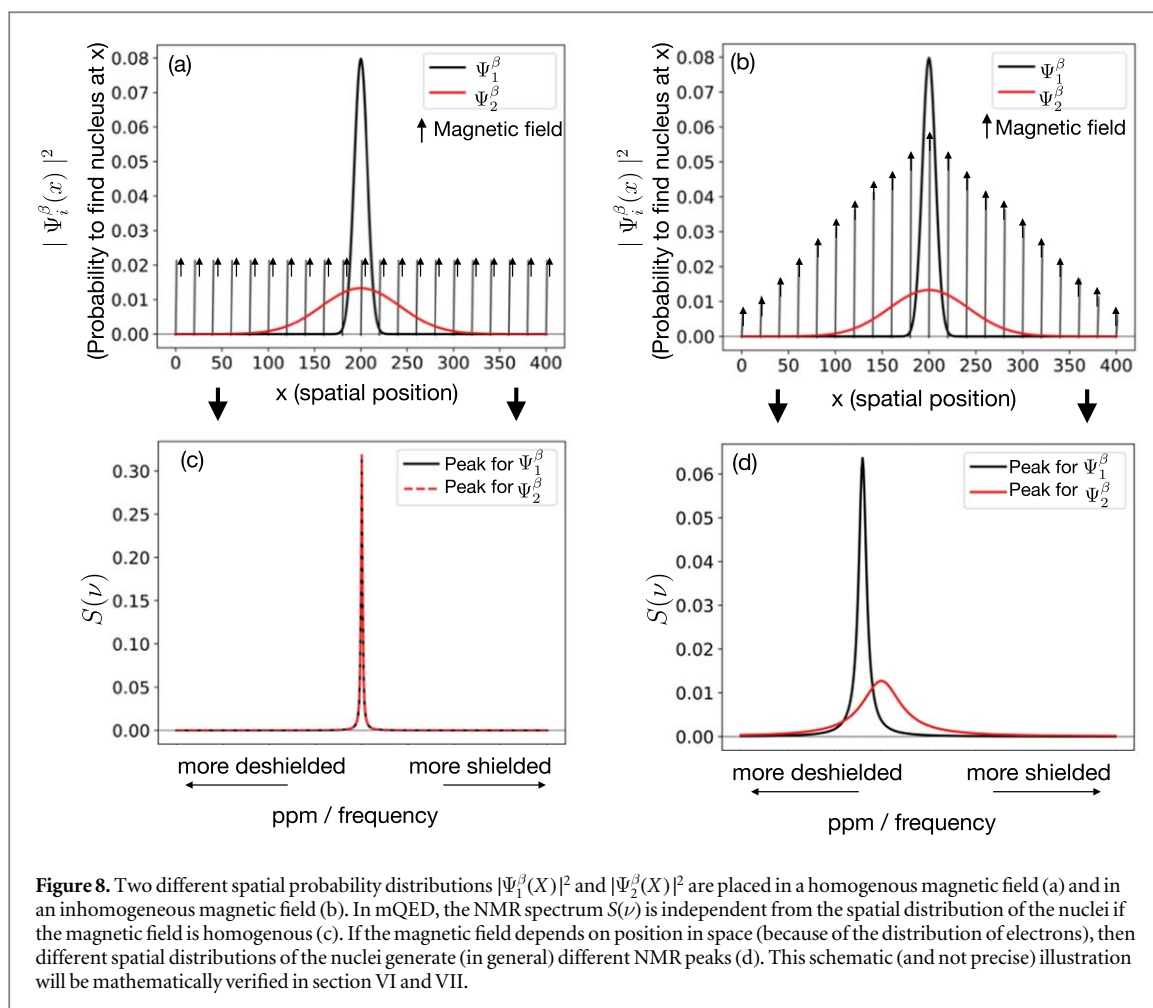


Figure 7. Molecules with a structure similar to that shown in the bottom end of the middle column typically generate temperature-dependent NMR spectra, as shown in the middle column. The thermal energy influences the spatial distribution of the methyl protons which causes a change not only in the positions of the NMR signals but also of the line shapes of the NMR signals. While the positions of the NMR signals can be calculated using quantum chemistry, conventional NMR theory cannot directly link the line shapes to the molecular structure. This is due to the fact that the spins are restricted to point positions and because thermalization is integrated phenomenologically by equation (4) instead of coupling the spins to the quantized electromagnetic field at finite temperatures. The result is that the underlying molecular structure can only be roughly reconstructed. This is different in mQED where the distribution of the spins is described by a continuous probability density $|\Psi^\beta(\theta)|^2$ (right column). The quantized EMF provides a natural thermalization such that all data points of the NMR spectrum (including the line shape) is directly connected to the underlying molecular structure. Hence, much more detailed investigations of the underlying molecular system become possible. The structural validity of this initially heuristic explanation is shown in sections VI, VII and VIII.

contrast to conventional NMR theory, where the N-Ph bond rotates with a certain frequency. The probability distribution $\rho^\beta(E_{rot}(\theta))$ from figure (6) is only a rough approximation for the more realistic, quantum mechanical probability distribution $|\Psi^\beta(\theta)|^2$. Hence, in a second second step, the distribution ρ^β can be slightly changed until the calculated NMR spectra agree with experimental NMR data. Hence, the probability distribution $|\Psi^\beta(X)|^2$ can be reconstructed from NMR data by using mQED at finite temperatures. A significant advantage of mQED is that the impact of the temperature on the molecular structure is taken into account much more realistically compared to conventional NMR theory. The result is that more realistic and more detailed molecular structures may be decoded from experimental NMR data. As a motivation for the presented method a heuristic illustration for a more detailed structure determination is outlined in figure 7. NMR spectra of such a molecule are not calculated in this document, but structural validity is shown.

In the zero temperature limit only the bond angle with the lowest energy is occupied (lowest row, (a) in figure 7). Such ground state structures are obtained from common quantum chemical calculations (like DFT). At low temperatures (second row from below, (b) in figure 7), where mainly low energetic bond angles are occupied (figure 6), the magnetic field generated by the ring is different for the green and the red marked methyl



group. Hence, both methyl groups have clearly distinct NMR signals. In contrast, conventional NMR theory assumes that the ring is slowly rotating with a fixed frequency. Hence, mQED and common NMR theory provide two different structures for the same situation. In mQED, bond angles with higher energies become more and more occupied with increasing temperature (third row from below, (c) in figure 7). Hence, each of the methyl groups comes closer to the opposite side of the ring. As a result both peaks on the spectrum come closer to each other. In conventional NMR theory, the rotation frequency is just slightly enhanced. However, in mQED there are still some bond angles which are nearly unoccupied ((b) in figure 6 and third row from below, (c) in figure 7). In NMR there is a specific temperature called "coalescence temperature" T_c , where the two peaks start to merge. At this temperature, also bond angles with higher energy are occupied but lower energetic bond angles are still preferred in mQED (black line in (c) of figure 6 and (d) in figure 7). This is not contained in conventional NMR theory, where the rotation frequency k is simply increased. At high temperature the two peaks merge completely and provide one sharp peak in the experimental NMR spectrum. In the interpretation of conventional NMR theory, the rotation frequency is much higher than the temporal resolution of the NMR spectrometer such that only one averaged signal is observed. The interpretation in mQED is that nearly all bonding angles are equally occupied in order to maximize the entropy. In this case, the resulting magnetic field is for both methyl groups the same, because it is spatially averaged. Hence, both methyl groups have the same chemical shift. The structural validity of this initially heuristic explanation is underpinned by an illustration (figure 8) which is mathematically verified in sections VI, VII and VIII.

In a region where the magnetic field is homogeneous the NMR peaks are independent from the spatial distribution of the nuclei ((a) and (c) in figure 8). Note that for high temperatures the distribution associated with T_3 in figure 6 generates a homogenous magnetic field in the region of both methyl groups ((e) in figure 7). Hence, both peaks are equal. However, if the magnetic field is inhomogeneous in the region of the methyl groups, because the spatial probability distribution depends on the bond angle (figures 6, 7 and 8), the methyl groups do not generate the same peak in the NMR spectrum $S(\nu)$. For relatively low temperatures the methyl groups are strongly localized in an inhomogeneous field. The NMR peaks will broaden with increasing delocalization of the methyl groups in an inhomogeneous magnetic field (figure 8) and hence have clearly distinct peaks. At the coalescence temperature T_c there are delocalized methyl groups in an inhomogeneous

magnetic field. With increasing temperature the magnetic field generated from the ring becomes more and more homogenous until both peaks merge to a single sharp peak at T_4 .

9. Conclusion

In this document it was shown how all data points of an NMR spectrum are mathematically connected via mQED at finite temperatures with the amplitude square $|\Psi^\beta(X)|^2$ of the nuclear wave function Ψ^β . Since $|\Psi^\beta(X)|^2$ represents the quantum statistical and temperature-dependent probability density on the continuous space \mathbb{R}^{3K} for the spatial distribution of the nuclei, the presented method may be used for a much more detailed reconstruction of molecular structures than possible with current methods. We briefly recall the weak points of conventional NMR theory which are improved by the presented method.

1. Conventional NMR theory based on Quantum Chemistry uses a discrete set of numbers (σ_i and J_{ij}) to approximate the continuous NMR spectrum. Hence, only the (punctiform) positions of NMR signals are directly connected with the molecular structure. However, also the line shapes of the signals contain information about the molecular structure.
2. So far, line shapes are investigated highly phenomenological such that only a rough notion of the investigated system can be obtained from this type of analysis.
3. Spin dynamics is conventionally based on the effective model which restricts the nuclei to fixed points in a lattice, requires phenomenological parameters for relaxation and delocalization and the initial state is at room temperature nearly temperature independent.

Explicit examples where the presented method should have advantages (should provide more molecular details) are the structure determination of furfural at different temperatures as shown in figure 1 or structure determinations of molecules similar to the ones shown in figure 7. Additional applications can be found in spin dynamics simulation for hyperpolarized MRI.

The main result (page 11) provides the structural application of molecular Quantum Electrodynamics and Quantum Statistical Mechanics in the algebraic reformulation to Nuclear Magnetic Resonance. Analytical and numerical calculations as well as comparisons with experimental NMR data showed the validity of this approach. Furthermore, wrong predictions of the effective spin model are corrected by the new approach (observation 1) and several striking advantages against established NMR theory were discussed. The presented method makes use of the physical approximation that the energy of an NMR pulse is too weak to change the molecular geometry which is also used in the effective spin model and obviously realistic for NMR. The important process of return to equilibrium is included in a natural and microscopic way instead phenomenologically as in equation (4). This provides a basis for a more detailed research towards optimized polarization transport and stable spin structures which are of basic interest in hyperpolarized MRI⁶⁷. Chemical shifts (magnetic shieldings) as well as spin-spin couplings occur naturally and must not be described effectively. Hence, quantum radiative corrections are naturally included in the calculated NMR spectrum.

The fundamental problem of performing numerical calculations with the infinite-dimensional radiation field at finite temperatures was solved by using a purified version of the Araki-Woods representation which served as a key element. The perturbation series equation (39) in combination with equation (41) generates combinations of sums and products of expectation values for individual spins instead of generating a complicated, shared matrix for the spins which increases exponentially with increasing number of spins. Thus, the presented method is not limited by the system size concerning the number of spins. Instead it is limited by the availability of a quantum chemical method which is able to calculate the electronic ground state for a given configuration X of the nuclei (see appendix). Thus, the developed method may be applied to molecular systems, which are currently investigated in chemistry, pharmacy, nanoscience or biomedicine.

Acknowledgments

K. T. acknowledges support by DFG-RFBR grant (HO 4604/3-1, No 19-53-12013). K. T. thanks his wife \mathcal{L}_t^β evin, Prof. Jan-Bernd Hövener and Prof. Klaus Fredenhagen for support and helpful discussions. This work is dedicated to Finn Them.

Author information

K. T. developed most of the present work autonomously before he was employed at UKSH and Kiel University. This concerns especially the mathematical structure and the software code.

Data availability statement

All data that support the findings of this study are included within the article (and any supplementary files).

Appendix

Mathematical structures that are required for the numerical calculations

A $*$ -morphism π between two $*$ -algebras \mathfrak{C} and \mathfrak{B} is defined as a mapping $\pi: A \in \mathfrak{C} \rightarrow \pi(A) \in \mathfrak{B}$ for all $A \in \mathfrak{C}$ such that $\pi(\alpha A + \gamma C) = \alpha\pi(A) + \gamma\pi(C)$, $\pi(AC) = \pi(A)\pi(C)$, and $\pi(A^*) = \pi(A)^*$ for all $A, C \in \mathfrak{C}$ and $\alpha, \gamma \in \mathbb{C}$. The kernel of a $*$ -morphism is given by the set $ker(\pi) = \{A \in \mathfrak{A}; \pi(A) = 0\}$. A representation is said to be faithful if, and only if, π_ω is a $*$ -isomorphism between \mathfrak{A} and $\pi(\mathfrak{A})$, i.e., if, and only if, $ker(\pi_\omega) = \{0\}$. A faithful representation satisfies $\|\pi_\omega(A)\| = \|A\|$, for all $A \in \mathfrak{A}$. If (\mathfrak{H}, π) is a representation of the C^* -algebra \mathfrak{A} and if \mathfrak{H}_0 is a subspace of \mathfrak{H} , then \mathfrak{H}_0 is said to be invariant under π if $\pi(A)\mathfrak{H}_0 \subseteq \mathfrak{H}_0$ for all $A \in \mathfrak{A}$. Hence, if \mathfrak{H}_0 is invariant under π and \mathfrak{H}^\perp is the orthogonal complement of \mathfrak{H}_0 , i.e., $\mathfrak{H}^\perp \doteq \{\xi \in \mathfrak{H}; \langle \xi, \psi \rangle = 0, \forall \psi \in \mathfrak{H}_0\}$, then we have $\langle \xi, \pi(A)\psi \rangle = 0$ for all $A \in \mathfrak{A}$ and all $\xi \in \mathfrak{H}^\perp, \psi \in \mathfrak{H}_0$. The group $\{\tau_t^{EM}\}_{t \in \mathbb{R}}$ provides the free field dynamics and the action is given by

$$W(f) \mapsto \tau_t^{EM}(W(f)) = W(e^{i\omega t f}) \quad \text{which implies} \quad \Phi(f) \mapsto \tau_t^{EM}(\Phi(f)) = \Phi(e^{i\omega t f}). \tag{58}$$

This is also known as Bogoliubov transformation. Note that the group $\{\tau_t^{EM}|t \in \mathbb{R}\}$ is not strongly continuous because $\|W(f) - W(g)\| = 2 \forall g \neq f$ and hence $(\mathcal{W}(\mathfrak{H}^r), \tau^{EM})$ is not a C^* -dynamical system.

Computational efforts for the numerical calculations involving complex molecules.

According to the main result of this article the time-dependent NMR signal of a molecule consisting of K nuclei and E electrons can written in the general form

$$\langle M^+ \rangle_\beta(t) = \int d^{3K} X d^{3E} X^e |\Psi^\beta(X)|^2 |\psi(X, X^e)|^2 \mathfrak{L}_t^\beta(A)(X, X^e), \tag{59}$$

where $\Psi^\beta \in L^2(\mathbb{R}^{3K}, \mathbb{C})$, $\psi \in L^2(\mathbb{R}^{3E}, \mathbb{C})$ and $\mathfrak{L}_t^\beta(A): \mathbb{R}^{3K} \times \mathbb{R}^{3E} \rightarrow \mathbb{C}$. Remember that $X = (\vec{x}_1, \dots, \vec{x}_K)$, $\vec{x}_i \in \mathbb{R}^3$ and $X^e = (\vec{x}^e_1, \dots, \vec{x}^e_E)$, $\vec{x}^e_j \in \mathbb{R}^3$. The integral kernel $\mathfrak{L}_t^\beta(A)(X, X^e)$ consists basically of expectation values of spins interacting with the quantized magnetic field. Due to the structure of the perturbation series equation (39) and (41), the structure of the purified Araki-Woods representation and the fact that the variables s_1, \dots, s_n and $t_1, \dots, t_{n'}$ are contained in exponential functions the integrals on s_1, \dots, s_n and $t_1, \dots, t_{n'}$ do not provide any challenge (at least for the first few orders). The used perturbation series does *not* generate any expectation values containing a matrix larger than a single spin operator which is due equation (36), (41) and (39). For example, if the investigated molecule contains only nuclei with spin 1/2, then the largest matrix which occurs in the calculation of the expectation values is of size 2×2 (or can be reduced to that size due to a tensor product with the unity operator). Hence, it is possible to determine the integral kernel $\mathfrak{L}_t^\beta(A)(X, X^e)$ analytically. Furthermore, due to the perturbation series the integral kernel can be decomposed into the following sum (where we neglect to denote the dependence of A on the right hand side and in the further text for simplicity)

$$\mathfrak{L}_t^\beta(A)(X, X^e) \cong f^\beta(t, X, X^e) = c_0 + c(t) + \sum_i f_i(t, \vec{x}_i) \tag{60}$$

$$+ \sum_{\substack{i,j=1,\dots,K \\ i \neq j}} f_{1ij}^\beta(t, \vec{x}_i, \vec{x}_j) + \sum_{\substack{i=1,\dots,K \\ j=1,\dots,E}} f_{2ij}^\beta(t, \vec{x}_i, \vec{x}^e_j) + \sum_{\substack{i,j=1,\dots,E \\ i \neq j}} f_{3ij}^\beta(t, \vec{x}^e_i, \vec{x}^e_j) \tag{61}$$

$$+ \sum_{\substack{i,l=1,\dots,K; i \neq l \\ j=1,\dots,E}} f_{4ijl}^\beta(t, \vec{x}_i, \vec{x}^e_j, \vec{x}_l) + \sum_{\substack{i=1,\dots,K \\ j,l=1,\dots,E; j \neq l}} f_{5ijl}^\beta(t, \vec{x}_i, \vec{x}^e_j, \vec{x}^e_l) + \dots \tag{62}$$

In the calculations in this document the constant c_0 contained information on the final state which describes the system after thermalization. The functions $c(t)$ and $f_i(t, \vec{x}_i)$ did not contribute and cancelled out. An example of an explicit part of $f_{1ij}^\beta(t, \vec{x}_i, \vec{x}_j)$ is shown in equation (56) and an example of an explicit part of $f_{2ij}^\beta(t, \vec{x}_i, \vec{x}^e_j)$ is shown in equation (57). Further terms of these integral kernels differ mainly by other combinations of the x-, y- and z-components of the spin and field operators. The computational effort for the evaluation of the integrals in equation (59) can be strongly reduced if we accept a common approximation that the wave function ψ (and potentially also Ψ^β) is given by tensor products of single electron wave functions as it is the case for the Slater determinant. In this case, the large number of integrals on the spatial coordinates $X^e = \vec{x}^e_1, \dots, \vec{x}^e_E$ of the E

electrons can be strongly reduced. For example

$$\int d^{3K} X d^{3E} X^e |\Psi^\beta(X)|^2 |\psi(X, X^e)|^2 f_{2ij}^\beta(t, \vec{x}_i, \vec{x}_j^e) = \int d^{3K} X d^{3E} X_j^e |\Psi^\beta(X)|^2 |\psi_j(X, \vec{x}_j^e)|^2 f_{2ij}^\beta(t, \vec{x}_i, \vec{x}_j^e). \quad (63)$$

The evaluation of these integrals can be done with any suitable standard numerical method. It remains to estimate up to which order the perturbation series needs to be calculated. For this purpose we use the fact that each term in the perturbation series has a clear physical interpretation that can also be verified mathematically:

1. $f_{1ij}^\beta(t, \vec{x}_i, \vec{x}_j)$ generates magnetic dipole-dipole interactions (direct couplings) between the nuclear spins i and j .
2. $f_{2ij}^\beta(t, \vec{x}_i, \vec{x}_j^e)$ generates a magnetic shielding on nuclear spin i caused by the electron j .
3. $f_{3ij}^\beta(t, \vec{x}_i^e, \vec{x}_j^e)$ generates magnetic interactions between spins of electron i and j .
4. $f_{4ijl}^\beta(t, \vec{x}_i, \vec{x}_j^e, \vec{x}_l)$ generates indirect spin-spin couplings between the nuclear spins i and l which is mediated via electron j
5. $f_{5ijl}^\beta(t, \vec{x}_i, \vec{x}_j^e, \vec{x}_l^e)$ generates different kinds of interactions between the nuclear spin i and electron spins j and l .

The above terms occur in the first few orders of the perturbation series and each higher order can generate additional coordinates. From this point of view it may seem to be sufficient to perform the calculations up to orders which generate terms that contain spatial coordinates of three particles or four particles. However, this is only an assumption. Since the multiplication operator f can be determined without numerical limitations up to high orders the numerical limitation of the presented method is primary given by the calculation of the amplitude square of the wave function $|\Psi^\beta(X)|^2 |\psi(X, X^e)|^2$ and the numerical integrations. The estimation of the electronic wave function ψ can be done with any common method of Quantum Chemistry. In agreement with conventional NMR theory the presented method assumes that the temperature dependence of the wave function ψ for electrons can be neglected due to high excitation energy of electrons in a molecule. This approximation is not necessary but reduces the computational complexity. Also the nuclear wave function Ψ^β may be calculated with any common method of Quantum Chemistry. Unfortunately, with current methods the exact calculation of Ψ^β can only be done for relative small and simple systems. However, this does not limit the presented method because only the amplitude square $|\Psi^\beta(X)|^2$ needs to be explored. Indeed, it is sufficient to initially approximate $|\Psi^\beta(X)|^2$ using any suitable method. For example, the PSE may be inserted into the classical Gibbs state. In further steps this approximation can be made more realistic, using artificial intelligence or manual adaptations, until there is sufficient agreement between the calculated spectrum and the experimental data.

The maintenance of gauge invariance can be quite a challenge in the conventional calculation of NMR parameters in Quantum Chemistry. This problem does not occur in the mQED perturbation series for the calculation of f^β , which is easily checked by the structure of equation (41) and (39). The only possibility where a challenge concerning the maintenance of gauge invariance may enter the presented method is in the calculation of ψ by conventional Quantum Chemistry. Here it should be noted that $\psi \in L^2(\mathbb{R}^{3E})$ is without spin degree of freedom which strongly simplifies the determination of ψ . Especially, for the calculation of ψ one is free to choose a Quantum Chemistry method which has no or little problems with the maintenance of gauge invariance. In addition, the presented method reduces problems concerning the maintenance of gauge invariance for Quantum Chemistry for the case were these problems occur because of the interaction with spin degrees of freedom. Due to the fact that each term can be calculated in parallel the author concludes that the presented method has basically the same numerical limitations as current methods of Quantum Chemistry used to determine ψ and the corresponding PSE.

Comparison of the magnetic shielding derived as temperature-dependent, effective parameter using Quantum Chemistry and the mQED approach in thermal equilibrium.

There is some formal similarity between the conventional approach of Quantum Chemistry to integrate the temperature, equation (3), and the results of mQED for the expectation value in thermal equilibrium. It is important to note that this similarity does *not* hold for the spin dynamics whose thermalization generates line shapes in the Fourier transformed spectrum. For simplicity we assume the six-dimensional case, $X = \vec{x}$ and $X^e = \vec{x}^e$. However, the $3n$ -dimensional case for n nuclei is in analogy. The effective parameter for the magnetic shielding of reference [13] can written as $\sigma_{\text{eff}}^\beta$, were

$$\sigma_{\text{eff}}^\beta \equiv \Delta^\beta \sigma + \sigma_{\text{eq}} = \int d^3x |\Psi^\beta(\vec{x})|^2 \sigma(\vec{x}). \quad (64)$$

Thus, $\sigma_{\text{eff}}^\beta$ is generated by an expectation value of the nuclear wave function with a multiplication operator $\sigma(\vec{x})$. Note that in the effective description only the nuclear wave function is temperature dependent, while $\sigma(\vec{x})$ is calculated at zero temperature. The expression a_φ^β (which has some similarities to $\sigma_{\text{eff}}^\beta$) derived from mQED in equation (51) can be written as

$$a_\varphi^\beta = \int d^3x |\Psi^\beta(\vec{x})|^2 \sigma_{\text{qed}}^{\beta\varphi}(\vec{x}), \quad (65)$$

with

$$\sigma_{\text{qed}}^{\beta\varphi}(\vec{x}) \doteq \int d^3x^e |\psi(\vec{x}, \vec{x}^e)|^2 b_{\varphi\beta}^{\text{zz}}(\vec{x}, \vec{x}^e), \quad (66)$$

where

$$b_{\varphi\beta}^{\text{zz}}(\vec{x}, \vec{x}^e) = \frac{g_s^2 \mu_B^2}{4} \int_0^\beta ds_1 \int_0^{s_1} ds_2 \int d^3k m_{\varphi\beta}^{\text{zz}}(\vec{x}, is_2, \vec{x}^e, is_1, \vec{k}). \quad (67)$$

The integral kernel $b_{\varphi\beta}^{\text{zz}}(\vec{x}, \vec{x}^e)$ provides the strength of the z-component of quantized magnetic field at the position \vec{x} of the nucleus, which is generated from the z-component of the electron spin at position \vec{x}^e . Hence, $\sigma_{\text{qed}}^{\beta\varphi}(\vec{x})$ may be interpreted as the averaged strength of the z-component of quantized magnetic field at the position \vec{x} of the nucleus. The average is done over all positions \vec{x}^e of the electron and weighted with the probability $|\psi(\vec{x}, \vec{x}^e)|^2$ to find the electron at position \vec{x}^e when the nucleus is at position \vec{x} . The integral in equation (65) on the coordinates of the nucleus weights the strength of the z-component of the quantized magnetic field at \vec{x} with the probability $|\Psi^\beta(\vec{x})|^2$ to find the nucleus at this position \vec{x} . Here is the similarity to the effective description, in which magnetic shielding, effectively derived using the classical magnetic field, is averaged \vec{x} with the probability $|\Psi^\beta(\vec{x})|^2$ to find the nucleus at this position \vec{x} .

The advantage of $\sigma_{\text{qed}}^{\beta\varphi}(\vec{x})$ of mQED is that finite temperature quantum fluctuations of the quantized magnetic field are included. It would be an interesting future work to investigate in which cases these fluctuations are relatively large or negligible. If these fluctuations are negligible for a system of interest, the mQED approach seems to provide for the *time-independent* investigation in *thermal equilibrium* no advantage over the effective description. However, an NMR spectrum is generated from the spin dynamics and thermalization as well as molecular motion are closely related to line shapes. Remember that for the spin dynamics there is no similarity between conventional NMR theory and the mQED description. This is mainly due to the phenomenological integration of thermalization in the effective description in equation (4).

Intermediate steps in the calculation of a_φ^β for the hydrogen atom.

According to the main result we calculate $\omega_M^\beta(\mathcal{L}_I^\beta(I^z))$ for thermal equilibrium ($t=0$). For the hydrogen atom we have

$$\omega_M^\beta(\mathcal{L}_0^\beta(I^z)) = \iiint_{\mathbb{R}^3} d^3x \iiint_{\mathbb{R}^3} d^3x^e |\Psi^\beta(\vec{x})|^2 |\psi_{100}(\vec{x}, \vec{x}^e)|^2 \hat{\omega}_{\text{SB}}^{I\beta}(\pi_{\text{SB}}^\beta \circ \tau_{P_0}^{\text{ISB}}(I^z))(\vec{x}, \vec{x}^e) \quad (68)$$

and need to know the explicit form of the integral kernel $\hat{\omega}_{\text{SB}}^{I\beta}(\pi_{\text{SB}}^\beta \circ \tau_{P_0}^{\text{ISB}}(I^z))(\vec{x}, \vec{x}^e)$. Step by step calculations provide

$$\begin{aligned} & \hat{\omega}_{\text{SB}}^{I\beta}(\pi_{\text{SB}}^\beta \circ \tau_{P_0}^{\text{ISB}}(I^z))(\vec{x}, \vec{x}^e) = \hat{\omega}_{\text{SB}}^{I\beta}(\pi_{\text{S}}(I^z) \otimes \hat{1})(\vec{x}, \vec{x}^e) \\ & = \underbrace{\text{Tr}(\rho_{\text{S}}^\beta I^z)}_{\text{0th order}} - \int_0^\beta ds_1 \int_0^{s_1} ds_2 \sum_{\alpha, \delta = x, y, z} \\ & \quad \times \left(\underbrace{\hat{\omega}_{\text{T,SB}}^\beta(\pi_{\text{SB}}^\beta(I^z), \hat{\gamma}_{is_2}^{\beta\text{SB}}(\gamma I^\alpha \otimes \Phi(b_\varphi^\alpha(\vec{x}))), \hat{\gamma}_{is_1}^{\beta\text{SB}}(g_s \frac{\mu_B}{\hbar} S^\delta \otimes \Phi(b_\varphi^\delta(\vec{x}^e)))}_{\text{2nd order}} \right. \\ & \quad \left. + \underbrace{\hat{\omega}_{\text{T,SB}}^\beta(\pi_{\text{SB}}^\beta(I^z), \hat{\gamma}_{is_2}^{\beta\text{SB}}(g_s \frac{\mu_B}{\hbar} S^\delta \otimes \Phi(b_\varphi^\delta(\vec{x}^e))), \hat{\gamma}_{is_1}^{\beta\text{SB}}(\gamma I^\alpha \otimes \Phi(b_\varphi^\alpha(\vec{x})))}_{\text{2nd order}} \right) + \dots \end{aligned} \quad (70)$$

and the dots represent 4th and higher order terms of the perturbation series equation (41). The first term of the integrand of the second order provides

$$\hat{\omega}_{\text{T,SB}}^\beta(\pi_{\text{SB}}^\beta(I^z), \hat{\gamma}_{is_2}^{\beta\text{SB}}(\gamma I^\alpha \otimes \Phi(b_\varphi^\alpha(\vec{x}))), \hat{\gamma}_{is_1}^{\beta\text{SB}}(g_s \frac{\mu_B}{\hbar} S^\delta \otimes \Phi(b_\varphi^\delta(\vec{x}^e))) = \gamma g_s \frac{\mu_B}{\hbar} (\text{Tr}(\rho_{\text{S}}^\beta I^z I^\alpha(is_2)) \text{Tr}(\rho_{\text{S}}^\beta S^\delta(is_1))) \quad (71)$$

$$- \text{Tr}(\rho_{\text{S}}^\beta I^z) \text{Tr}(\rho_{\text{S}}^\beta I^\alpha(is_2)) \text{Tr}(\rho_{\text{S}}^\beta S^\delta(is_1)) \quad (72)$$

$$\times \omega_{EM}^{\beta}(\tau_{is_2}^{EM}(\Phi(b_{\varphi}^{\alpha}(\vec{x}))))\tau_{is_1}^{EM}(\Phi(b_{\varphi}^{\gamma}(\vec{y}))). \quad (73)$$

The second term of the integrant of the second order provides an analogous expression, where just some indices are changed. Thus, we have

$$\mathfrak{L}_0^{\beta}(I^z) \approx \text{Tr}(\rho_S^{\beta} I^z) - \gamma_{GS} \frac{\mu_B}{\hbar} \text{Tr}(\rho_S^{\beta} S^z) \int_0^{\beta} ds_1 \int_0^{s_1} ds_2 m_{\varphi\beta}^{zz}(\vec{x}, is_2, \vec{x}^e, is_1, \vec{k}) + \dots \quad (74)$$

Using the high temperature approximation for ρ_S^{β} one obtains the results shown in equation (49) and (51). Note that here it can be seen that no large matrix is generated even for large molecules because of the tensor product structure in equation (36).

NMR signal of a helium atom.

The dynamic calculations for the hydrogen atom of the main manuscript are compared to the case of a helium atom in order to get a first notion for more complex systems. If electron-electron interactions are neglected the 1s orbital ψ_{100}^Z of an atom with nuclear charge Z is given by

$$\psi_{100}^Z(\vec{x}, \vec{x}^e) = \left(\frac{Z^3}{\pi a_0^3} \right)^{1/2} e^{-\frac{Z|\vec{x}-\vec{x}^e|}{a_0}}. \quad (75)$$

We have $Z = 1$ for hydrogen and $Z = 2$ for helium. In the case of a hydrogen atom the integral kernel f_H^{β} of equation (60) has up to 6 spatial variables and we may write

$$f_H^{\beta}(t, \vec{x}, \vec{x}^e) = f_{H,2}^{\beta}(t, \vec{x}, \vec{x}^e) + \dots, \quad (76)$$

where the dots denote higher order terms. Hence, the NMR signal for the hydrogen atom, $\langle M_H^+ \rangle_{\beta}(t)$, may be approximated by

$$\langle M_H^+ \rangle_{\beta}(t) \approx \int d^3x d^3x^e |\Psi_H^{\beta}(\vec{x})|^2 |\psi_{100}^1(\vec{x}, \vec{x}^e)|^2 f_{H,2}^{\beta}(t, \vec{x}, \vec{x}^e) \quad (77)$$

For the Helium atom one finds

$$f_{He}^{\beta}(t, \vec{x}, \vec{x}_1^e, \vec{x}_2^e) \approx f_{He,2}^{\beta}(t, \vec{x}, \vec{x}_1^e) + f_{He,2}^{\beta}(t, \vec{x}, \vec{x}_2^e) + f_{He,3}^{\beta}(t, \vec{x}_1^e, \vec{x}_2^e) + f_{He,5}^{\beta}(t, \vec{x}, \vec{x}_1^e, \vec{x}_2^e) + \dots \quad (78)$$

The functions $f_{H,2}$ and $f_{He,2}$ just differ by a factor of γ_{He}/γ_H . For the electrons of the helium atom we may assume the symmetric wave function $\psi_{He}^S = \psi_{100}^2 \otimes \psi_{100}^2$ for the spatial degrees of freedom,

$$\psi_{He}^S(\vec{x}, \vec{x}_1^e, \vec{x}_2^e) = \psi_{100}^2(\vec{x}, \vec{x}_1^e) \psi_{100}^2(\vec{x}, \vec{x}_2^e). \quad (79)$$

Of course, the index 2 denotes $Z = 2$ and not the square. As mentioned above the spin operators are already contained as expectation values in the multiplication operator f . We derive

$$\int d^3x d^3x_1^e d^3x_2^e |\Psi_{He}^{\beta}(\vec{x})|^2 |\psi_{He}^S(\vec{x}, \vec{x}_1^e, \vec{x}_2^e)|^2 (f_{He,2}^{\beta}(t, \vec{x}, \vec{x}_1^e) + f_{He,2}^{\beta}(t, \vec{x}, \vec{x}_2^e)) \quad (80)$$

$$= \int d^3x |\Psi_{He}^{\beta}(\vec{x})|^2 \left(\int d^3x_1^e |\psi_{100}^2(\vec{x}, \vec{x}_1^e)|^2 f_{He,2}^{\beta}(t, \vec{x}, \vec{x}_1^e) + \int d^3x_2^e |\psi_{100}^2(\vec{x}, \vec{x}_2^e)|^2 f_{He,2}^{\beta}(t, \vec{x}, \vec{x}_2^e) \right) \quad (81)$$

$$= 2 \int d^3x d^3x^e |\Psi_{He}^{\beta}(\vec{x})|^2 |\psi_{100}^2(\vec{x}, \vec{x}^e)|^2 f_{He,2}^{\beta}(t, \vec{x}, \vec{x}^e) \quad (82)$$

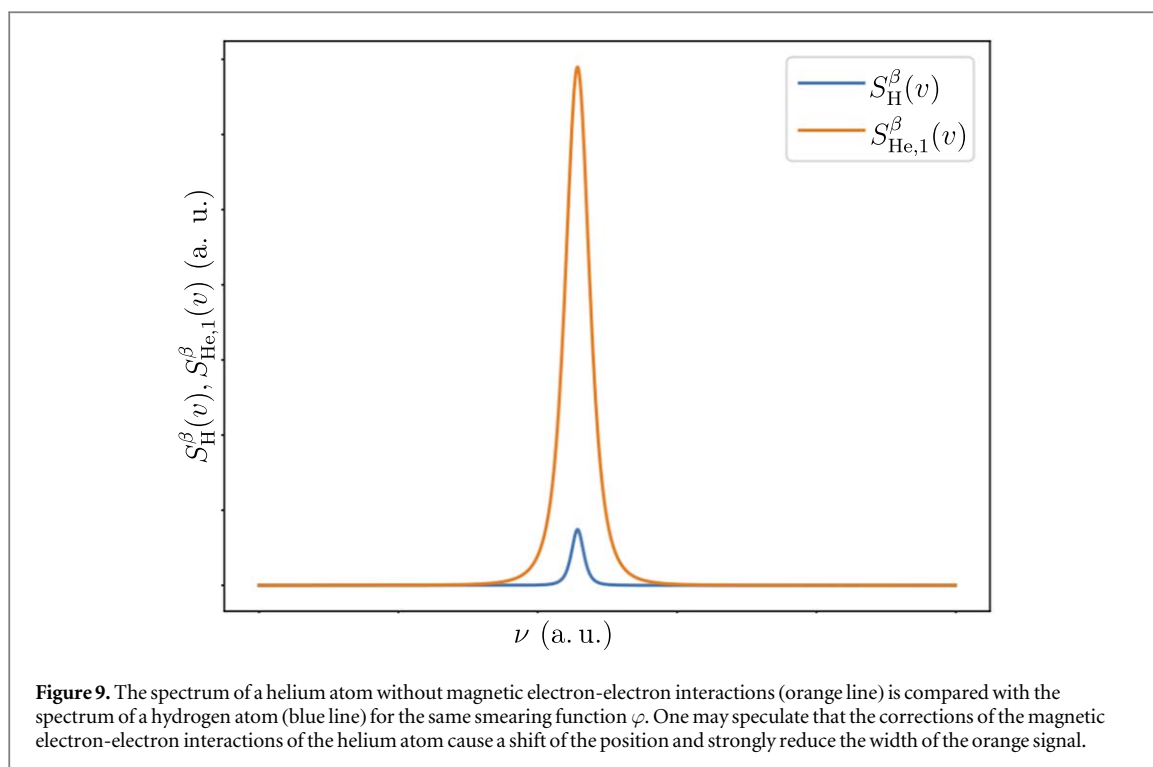
and find for the NMR signal $\langle M_{He}^+ \rangle_{\beta}(t)$ of the helium atom

$$\langle M_{He}^+ \rangle_{\beta}(t) \approx 2 \underbrace{\int d^3x d^3x^e |\Psi_{He}^{\beta}(\vec{x})|^2 |\psi_{100}^2(\vec{x}, \vec{x}^e)|^2 f_{He,2}^{\beta}(t, \vec{x}, \vec{x}^e)}_{\doteq \langle M_{He,1}^+ \rangle_{\beta}(t)} \quad (83)$$

$$+ \int d^3x d^3x_1^e d^3x_2^e |\Psi_{He}^{\beta}(\vec{x})|^2 |\psi_{He}^S(\vec{x}, \vec{x}_1^e, \vec{x}_2^e)|^2 (f_{He,3}^{\beta}(t, \vec{x}_1^e, \vec{x}_2^e) + f_{He,5}^{\beta}(t, \vec{x}, \vec{x}_1^e, \vec{x}_2^e)) + \dots \quad (84)$$

The first term, denoted by $\langle M_{He,1}^+ \rangle_{\beta}(t)$, is very similar to the signal $\langle M_H^+ \rangle_{\beta}(t)$ of the hydrogen atom. It just differs by a factor of 2, which arises because 2 electrons contribute, the value $Z = 2$ of the nuclear charge and the value γ_{He}/γ_H . The function $\langle M_{He,1}^+ \rangle_{\beta}(t)$ describes the NMR signal of a helium atom without electric and magnetic electron-electron interactions. The latter ones are generated by $f_3^{\beta}(t, \vec{x}_1^e, \vec{x}_2^e)$ and $f_5^{\beta}(t, \vec{x}, \vec{x}_1^e, \vec{x}_2^e)$.

Furthermore, one finds as in the case of hydrogen that $\langle M_{He,1}^+ \rangle_{\beta}(t)$ is independent of Ψ_{He}^{β} . This is because a single nucleus in a homogenous external field is considered and it can be found mathematically by the multiplication of $m_{\varphi\beta}^{zz}(\vec{x}, is_2, \vec{x}^e, is_1, \vec{k})$ with the exponential of the Fourier transform for Ψ_{He}^{β} . As mentioned above, the NMR signal of a molecule with two or more nuclei explicitly depends on Ψ^{β} . In this document we do not calculate the corrections of the magnetic electron-electron interactions for $\langle M_{He}^+ \rangle_{\beta}(t)$ but compare the spectra $S_{He,1}^{\beta}(t)$ and $S_H^{\beta}(t)$ (figure 9) which are generated as Fourier transformations of $\langle M_{He,1}^+ \rangle_{\beta}(t)$ with $\langle M_H^+ \rangle_{\beta}(t)$ according to equation (47). Based on the numerical comparison of the spectra it seems to be important to include the corrections of magnetic electron-electron interactions provided by $f_3^{\beta}(t, \vec{x}_1^e, \vec{x}_2^e)$ and $f_5^{\beta}(t, \vec{x}, \vec{x}_1^e, \vec{x}_2^e)$. One may expect that these corrections shift the position of the peak and make the peak much thinner. Note that the



unpaired electron of the hydrogen atom speeds up the thermalization process and a faster decay of the NMR signal in the time-domain corresponds to a broader width of the NMR peak in the frequency domain.

ORCID iDs

Kolja Them  <https://orcid.org/0000-0002-5512-0910>

References

- [1] Schmidt M *et al* 1993 *J. Comput. Chem.* **14** 1347
- [2] Wagner J *et al* 2013 *Acta Neuropathol.* **125** 795
- [3] Ionin B, Ershov B A and Aleksandrovich B 1983 *NMR Spectroscopy in Organic Chemistry* (Berlin: Springer)
- [4] Holzgrabe U 2017 *NMR Spectroscopy in Pharmaceutical Analysis* ed U Holzgrabe, I Wawer and B Diehl (Amsterdam: Elsevier) 9780444531753
- [5] He Y, He L, Lan P, Wang B, Li L, Zhu X, Cao W and Lu P 2019 *Phys. Rev. A* **99** 053419
- [6] Holzschuh M and von Quantenmechanische Berechnung 2016 NMR chemischen Verschiebungen und indirekten Spin-Spin Kopplungskonstanten von Carbokationen *Ph.D. Thesis* Universität Ulm (<https://doi.org/10.18725/OPARU-4183>) (<https://oparu.uni-ulm.de/xmlui/handle/123456789/4222>)
- [7] Becker E D 1999 *High Resolution NMR: Theory and Chemical Applications* (Amsterdam: Elsevier) 9780120846627
- [8] Cremer D, Olsson L, Reichel F and Kraka E 1993 *Isr. J. Chem.* **33** 369
- [9] Kaupp M, Bühl M and Malkin V G 2006 *Calculation of NMR and EPR Parameters: Theory and Applications* (New York: Wiley) 978-3-527-30779-1
- [10] Cordier F and Grzesiek S 2002 *J. Mol. Biol.* **317** 739
- [11] Bain A D, Duns G, Rathgeb F and Vanderkloet J 1995 *The Journal of Physical Chemistry* **99** 17338
- [12] Bain A D and Hazendonk P 1997 *The Journal of Physical Chemistry A* **101** 7182
- [13] Faber R, Kaminsky J and Sauer S P 2016 *Gas Phase NMR* (London: Royal Society of Chemistry) pp 218–66
- [14] Kovrigin E L 2012 *J. Biomol. NMR* **53** 257
- [15] Waudby C A, Ramos A, Cabrita L D and Christodoulou J 2016 *Sci. Rep.* **69** 24826
- [16] Niklasson M, Otten R, Ahlner A, Andresen C, Schlagnitweit J, Petzold K and Lundström P 2017 *J. Biomol. NMR* **69** 3
- [17] Cheshkov D, Sheberstov K, Sinityn D and Chertkov V 2018 *Special Issue: Software Tools and Tutorials in Liquid State NMR* **56** 449
- [18] Pravdivtsev A N and Hövener J-B 2019 *Chem. Eur. J* **25** 7580
- [19] Perrin C L and Dwyer T J 1990 *Chem. Rev.* **90** 935
- [20] Olsson S and Noe F 2017 *J. Am. Chem. Soc.* **139** 200
- [21] Abergel D and Palmer A G 2018 *ChemPhysChem* **5** 787
- [22] Edwards L J, Savostyanov D, Welderufael Z, Lee D and Kuprov I 2014 *J. Magn. Reson.* **243** 107
- [23] Bak M, Rasmussen J T and Nielsen N C 2011 *J. Magn. Reson.* **213** 366
- [24] Helgaker T, Watson M and Handy N C 2000 *J. Chem. Phys.* **113** 9402
- [25] Špirtović-Halilović S, Salihović M, Trifunović S, Roca S, Veljović E, Osmanović A, Vinković M and Završnik D 2014 *J. Serb. Chem. Soc.* **79** 1405

- [26] Autschbach J and Zheng S 2009 *Annual Reports on NMR Spectroscopy* **67** 1
- [27] Demissie T B 2017 *J. Chem. Phys.* **147** 174301
- [28] Cheng L, Xiao Y and Liu W 2009 *J. Chem. Phys.* **130** 144102
- [29] Romero R H and Aucar G A 2002a *Phys. Rev. A* **65** 053411
- [30] Romero R and Aucar G 2002b *Int. J. Mol. Sci.* **3** 914
- [31] Yerokhin V A, Pachucki K, Harman Z and Keitel C H 2011 *Phys. Rev. Lett.* **107** 043004
- [32] Gimenez C A, Koziol K and Aucar G A 2016 *Phys. Rev. A* **93** 032504
- [33] Aucar G A, Romero R H and Maldonado A F 2010 *Int. Rev. Phys. Chem.* **29** 1
- [34] Aucar G A 2008 *Concepts in Magnetic Resonance Part A: An Educational Journal* **32** 88
- [35] Lounila J and Diehl P 1984 *Mol. Phys.* **52** 827
- [36] Them K, Stapelfeldt T, Vedmedenko E Y and Wiesendanger R 2013 *New J. Phys.* **15** 013009
- [37] Farrarher S W, Jara H, Chang K J, Ozonoff A and Soto J A 2006 *Journal of Magnetic Resonance Imaging: An Official Journal of the International Society for Magnetic Resonance in Medicine* **24** 1333
- [38] Kuprov I 2011 *J. Magn. Reson.* **209** 31
- [39] Kleier D A and Binsch G 1970 *Journal of Magnetic Resonance (1969)* **3** 146
- [40] Ruggenthaler M, Tancogne-Dejean N, Flick J, Appel H and Rubio A 2018 *Nature Reviews Chemistry* **2** 0118
- [41] Schäfer C, Ruggenthaler M and Rubio A 2018 *Phys. Rev. A* **98** 043801
- [42] Mück M 2005 *Thermal Relaxation for Particle Systems in Interaction with Several Bosonic Heat Reservoirs* edn 1 (BoD-Books on Demand GmbH)
- [43] Santana A E d, Neto A M, Vianna J and Khanna F 2000 *Physica A* **280** 405
- [44] Ojima I 1981 *Ann. Phys.* **137** 1
- [45] Santana A E d, Neto A M, Vianna J and Khanna F C 1999 *Int. J. Theor. Phys.* **38** 641
- [46] Bratteli O and Robinson D W 1979 *English Operator Algebras and Quantum Statistical Mechanics I* (New York: Springer)
- [47] Bratteli O and Robinson D W 1981 *English Operator Algebras and Quantum Statistical Mechanics II* (Berlin, Heidelberg: Springer)
- [48] Buchholz D 1982 *Commun. Math. Phys.* **85** 49
- [49] Fredenhagen K and Lindner F 2014 *Commun. Math. Phys.* **332** 895
- [50] Haag R 1993 *Local Quantum Physics: Fields, Particles, Algebras* (Berlin: Springer)
- [51] Brunetti R, Dappiaggi C, Fredenhagen K and Yngvason J 2015 *Advances in Algebraic Quantum Field Theory* (Berlin: Springer)
- [52] Amour L and Nourrigat J 2015 arXiv:1512.08429
- [53] Amour L, Jager L and Nourrigat J 2017 arXiv:1709.02771
- [54] Drago N, Hack T-P and Pinamonti N 2017 *Annales Henri Poincaré* vol 18 (Berlin: Springer) pp 807–68
- [55] Araki H and Woods E 1963 *J. Math. Phys.* **4** 637
- [56] Dereziński J and Jakšić V 2003 *Ann. Henri Poincaré* **4** 739
- [57] Lieb E H and Loss M 2005 *The Stability of Matter: From Atoms to Stars* (Berlin: Springer) pp 709–21
- [58] Lieb E H and Loss M 2004 *Commun. Math. Phys.* **252** 477
- [59] Them K 2014 *Applications of the C^* -algebraic Reformulation of Quantum Statistical Mechanics to the Description of Experimentally Investigated spin systems.*, Dissertation (University of Hamburg) (<https://ediss.sub.uni-hamburg.de/handle/ediss/5693>)
- [60] Them K 2014 *Phys. Rev. A* **89** 022126
- [61] Them K, Vedmedenko E Y, Fredenhagen K and Wiesendanger R 2015 *J. Phys. A: Math. Theor.* **48** 075301
- [62] Knopp T, Them K, Kaul M and Gdaniec N 2015 *Phys. Med. Biol.* **60** L15 multi-patch, article
- [63] Them K, Kaul M G, Jung C, Hofmann M, Mummert T, Werner F and Knopp T 2016a *IEEE Trans. Med. Imaging* **35** 893
- [64] Them K, Salamon J, Swargulski P, Sequeira S, Kaul M G, Lange C, Ittrich H and Knopp T 2016b *Phys. Med. Biol.* **61** 3279
- [65] K. T. in discussion with Klaus Fredenhagen, (February 2020)
- [66] Wang J, Dong H and Li S-W 2018 *Phys. Rev. A* **97** 013819
- [67] Them Kolja *et al* 2020 (<https://arxiv.org/ftp/arxiv/papers/2012/2012.03626.pdf>)